ANTIANDROGEN-EQUIPPED GENISTEIN CONJUGATES FACILITATE ANDROGEN RECEPTOR DOWNREGULATION IN PROSTATE CANCER

A Thesis
Presented to
The Academic Faculty

by

Alex George

In Partial Fulfillment
of the Requirements for the Degree
B.S. in Biochemistry with Research Option in the
School of Chemistry and Biochemistry

Georgia Institute of Technology
April 2016

ANTIANDROGEN-EQUIPPED GENISTEIN CONJUGATES FACILITATE ANDROGEN RECEPTOR DOWNREGULATION IN PROSTATE CANCER

Approved by:

Dr. Adegboyega K. Oyelere, Advisor
School of Chemistry and Biochemistry
Georgia Institute of Technology

Dr. Donald F. Doyle
School of Chemistry and Biochemistry
Georgia Institute of Technology

Dr. Angus P. Wilkinson
School of Chemistry and Biochemistry
Georgia Institute of Technology

Date Approved: May 5, 2016

ACKNOWLEDGEMENTS

I thank my advisor, Dr. Oyelere as well as the members of the Oyelere group for their continued support and mentorship throughout the completion of my research. I thank Idris Raji for his expertise and mentorship in addition to his significant contributions to the molecular biology components of this project. I thank Dr. Subhashish Tapadar for his mentorship in synthesis and I also thank Dr. Doyle for his advice in writing this thesis.

In addition, I would like to take a moment to thank my entire family, especially my parents Benny and Jessy as well as my siblings Josh and Christine for their continued support throughout my life and my undergraduate career.

TABLE OF CONTENTS

LIST OF FIGURES

LIST OF SYMBOLS AND ABBREVIATIONS

PCa	Prostate Cancer
AR	Androgen Receptor
HSP90	Heat Shock Protein 90
DHT	Dihydroxytestosterone
AREs	Androgen-Response Elements
ADT	Androgen Deprivation Therapy
LHRH	Luteinizing Hormone-Release Hormone
CRPC	Castration Resistant Prostate Cancer
TRKs	Tyrosine Receptor Kinases
MAPKs	Mitogen Activated Protein Kinase Signaling Pathways
VEGF	Vascular Endothelial Growth Factor
MMP	Matrix Metalloprotease
ECM	Extracelluar Matrix
TSGs	Tumor Suppressor Genes
HATs	Histone Acetyltransferases
hTERT	Human Telomerase Reverse Transcriptase
PSA	Prostate Specific Antigen
UPS	Ubiquitin Protease System
HDAC	Histone Deacetylase
SARD	Selective Androgen Receptor Degrader
PEG	Polyethylene Glycol
IC_{50}	Half Maximal Inhibitory Concentration
DMSO	Dimethyl sulfoxide

SUMMARY

Prostate cancer is the second most leading cause of cancer-related death among American men. The expression of androgen receptor protein has been established by numerous studies as a main driving force for the progression of prostate cancer. In an effort to combat this disease, potent compounds such as genistein have been identified to have significant anti-cancer activity and androgen receptor modulation in prostate cancer cells. Furthermore, studies have shown that antiandrogen ligands may be functionalized with hydrophobic moieties to selectively degrade androgen receptor protein *in vitro*. Building upon these findings, this study explores the efficacy of a bifunctional molecule; specifically a combination of a potent, non-steroidal enzalutamide-derived antiandrogen with genistein acting as a partially hydrophobic degradation tag. Preliminary cell viability studies have identified a promising lead compound (compound 9b) within the synthesized conjugates. This compound exhibits potent inhibition of cell growth in androgen sensitive LNCaP cells (IC_{50} = 1.44 ± 0.9 μM), and androgen insensitive DU145 cells (IC_{50} = 3.38 ± 0.9 μM). Western immunoblotting studies confirm the dose-dependent degradation of androgen receptor and cell cycle analyses indicate S-phase arrest with the treatment of compound 9b. While preliminary immunoblotting studies suggest the degradation of androgen receptor is mediated by the ubiquitin protease system, further studies must be carried out to validate these preliminary results. Future studies include looking into androgen receptor binding efficacy with the addition of the genistein moiety and the effect of the target compounds on the metastatic potential of bone-derived (PC3) prostate cancer cells.

CHAPTER 1

INTRODUCTION

I. OVERVIEW

Among American men, prostate cancer (PCa) is the second most leading cause of cancer-related death and accounts for nearly 240,000 new cases each year [1, 2]. AR expression has been shown by numerous studies to be vital in prostate cancer cell progression [3]. Genistein (Figure 1.3A), a natural soy isoflavone, is among the most potent phytogestrogens to have beneficial pharmacological effects in animal cells and also exhibit antitumor activity [4]. Genistein has the potential to become a powerful therapeutic against prostate cancer due to many properties that work in concert to exhibit anti-proliferative activity in cancer cells [4]. Previous studies have primarily focused on elucidating the mechanisms by which genistein works to suppress cancer growth [5-10]. Recent research in the area of drug design has shown that the incorporation of multiple pharmaceutical moieties on a single molecule has the potential to enhance drug efficacy and specificity to prostate cancer cells via androgen receptor (AR) binding [11] and the subsequent utilization of cellular machinery such as the ubiquitin protease system (UPS) to selectively degrade AR protein [12-14]. With regard to these findings, a novel pharmaceutical design incorporating genistein may prove to be a potent therapeutic for prostate cancer while also reducing AR expression.

II. THE ROLE OF ANDROGEN RECEPTOR IN PROSTATE CANCER

The androgen receptor (AR) is involved in the normal function of the prostate and other tissues and is important in the progression of PCa [15]. In its unbound state, AR is a steroid hormone receptor found in the cytoplasm associated with heat shock proteins (HSP-90), cytoskeletal proteins, and other chaperones [16]. After binding to one of its natural ligands (dihydroxytestosterone (DHT) or testosterone), AR undergoes a conformational change which results in homodimerization, followed by nuclear translocation, DNA binding, and the transcription of AR regulated genes [17]. The AR regulates gene expression via binding to androgen-response elements (AREs) in proximity to genes directly transcribed by the AR [15].

For patients with early stage prostate cancer, androgen deprivation therapy (ADT) is often employed as a first-line therapy in the form of antiandrogens or luteinizing hormone-releasing hormone (LHRH) agonists. While most patients respond well to ADT, many of these patients will become refractory to treatment and develop castration resistant PCa (CRPC) [18]. Several studies have shown that the frequency of AR mutations is higher in CRPC, which draws attention to the role of AR in PCa progression [19, 20]. AR mutations have been shown to result in the conversion of several AR antagonists (e.g. bicalutamide, nilutamide, enzalutamide) to agonists [21-23] and also allow for the receptor to be activated by a broad range of ligands [24-26]. The importance of AR expression in CRPC progression is clear as AR expression is nearly 6-fold higher in CRPC compared to hormone-sensitive PCa [27]. As such, numerous second-line therapies (i.e. enzalutamide, abiraterone) treat CRPC by targeting androgen synthesis and/or AR regulation/signaling [28-30].

III. GENISTEIN ACTIVITY

Several studies have been performed to characterize the mechanisms that genistein uses to inhibit proliferative activity in cancer cells. Cao et. al showed that genistein can inhibit the activity of tyrosine receptor kinases (TRKs) and subsequently inhibit mitogen activated protein kinase signaling pathways (MAPKs) [8, 31]. Genistein actively inhibits the phosphorylation of TRK, thereby inhibiting the TRK signal transduction pathway (TRK → Raf →MEK → ERK/p38). Sasamura et. al identified the anti-proliferative effect of the inhibition of TRK by genistein in human renal cell carcinoma [8]. Studies have also shown that genistein can inhibit the NF-kB pathway in prostate cancer cells [5, 7]. Li et. al indicated that inhibition of NF-kB by genistein is linked to the Akt signaling pathway for cell survival. Immunoprecipitation and kinase assays have shown that genistein specifically inhibits Akt kinase activity and also epidermal growth factor induced activation of Akt in prostate cancer cells [7]. Furthermore, this inhibition was only observed in tumorigenic prostate cancer cells, but not prostate epithelial cells [7]. Davis et. al showed that genistein specifically prevents NF-kB activation by DNA-damaging agents and also suggested that the inhibition of NF-kB may be genistein's mechanism of inducing apoptosis in cancer cells [5].

In the metastasis of cancer, vascularization is a key step in sustaining tumor growth and allowing cancer cells to migrate. Results by Su. et. al, genistein has been shown to inhibit angiogenesis in human bladder cancer cells [9]. It was reported that genistein exhibited a dose-dependent inhibition of vascular endothelial growth factor (VEGF), platelet-derived growth factor, and matrix metalloprotease-2 and 9 (MMP 2 and 9) [9]. The suppression of MMP 2 and 9 shows that genistein helps to suppress the

degradation of the extracellular matrix (ECM) needed for metastasis as well. It was also found that angiogenesis inhibitors such as endostatin, angiostatin, and thrombospodin-1 were up-regulated [9].

The development of prostate cancer is often linked to the accumulation of genetic and epigenetic modifications that result in the silencing of tumor suppressor genes (TSGs). It has been shown that genistein increases the expression of several histone acetyltransferases (HATs) in LNCaP and DuPro prostate cancer cell lines as well as normal epithelial prostate cancer cells [32]. The increased expression of HATs allow for the increased acetylation of histones H3 and H4 which increases the transcription of p21 and p16, genes that induce cell cycle arrest and apoptosis [32]. Furthermore, increased H3K9 acetylation indicated the re-expression of important tumor suppressor genes such as PTEN, p53, CYLD and FOXO3a [33]. Jagadeesh et. al also shows that genistein affects telomerase activity [6]. Telomerase activity is essential for cells to gain immortality and sustained proliferation as it is responsible for the integrity of the genome. Genistein was found to down-regulate the expression of human telomerase reverse transcriptase (hTERT) in prostate cancer cells [6].

Genistein has also been shown to decrease AR protein, mRNA levels, and binding to AREs which resulted in the reduction of androgen-mediated transcriptional activation of prostate specific antigen (PSA) in androgen-dependent cells [34, 35]. Furthermore, the estrogenic activity of genistein downregulates HDAC6-HSP90 chaperone function and has been attributed to the increased ubiquitination of AR and subsequent degradation by the UPS in PCa cells, thereby decreasing AR protein levels [36].

IV. COMBINATORIAL TREATMENTS WITH GENISTEIN

Combinational therapies have long been used in the treatment of cancer to gain increased drug performance. Phillip et. al has shown that genistein cooperates with HDAC inhibitor vorinostat to induce apoptosis in prostate cancer cells [37]. A combination of the epigenetic effects of genistein (increased HAT1 activity and H3K9 acetylation) and HDACi led to increased levels of apoptosis via the effective transcription of TSGs [37]. Another study by Gryder et. al couples an AR inhibiting nilutamide moiety (antiandrogen) with vorinostat to selectively target and accumulate the pharmaceutical in prostate cancer cells [11]. This mechanism of action utilizes AR's affinity for nuclear localization (Figure 1.1) to allow vorinostat to accumulate in cancerous cells and induce epigenetic modifications while also inhibiting AR.

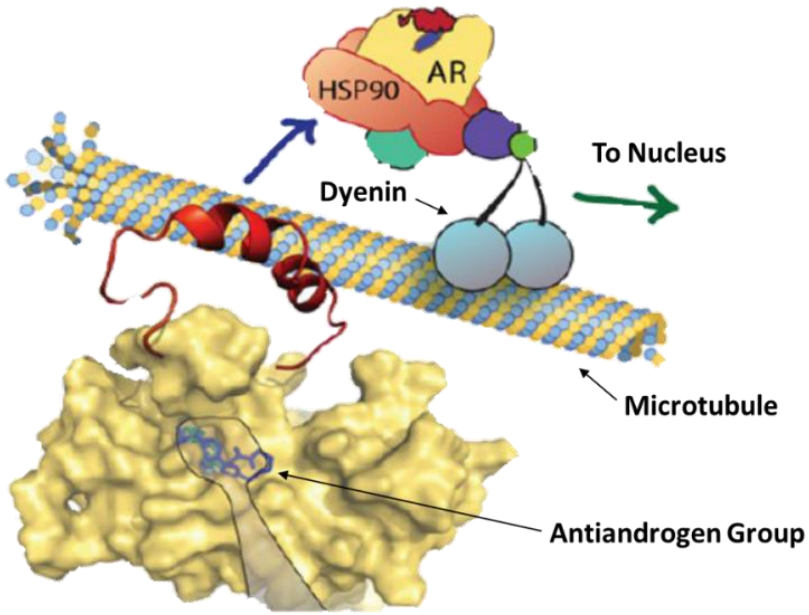

Figure 1.1 *An antiandrogen group binds to AR and is transported to nucleus along microtubules via dynein proteins[11].*

V. SELECTIVE PROTEIN DEGRADATION AND PHARMACEUTICAL DESIGN

The selective degradation of clinically relevant proteins such as AR represents a novel strategy that could offer a direct solution to the progression of PCa. Postulating that increased AR protein expression drives the development of CRPC, we pursued a bifunctional, pharmaceutical design that would incorporate the cancer killing properties of an antiandrogen and genistein, and possibly act as a selective androgen receptor degrader (SARD). Various studies have demonstrated that hydrophobic tagging via a small, bifunctional molecule is a viable strategy for the post-translational targeting of AR and other proteins for degradation [12-14]. An example of a well-characterized SARD is given by Figure 1.2. In essence, this hydrophobic tagging simulates a misfolded protein which is then processed and degraded by the UPS [14, 38].

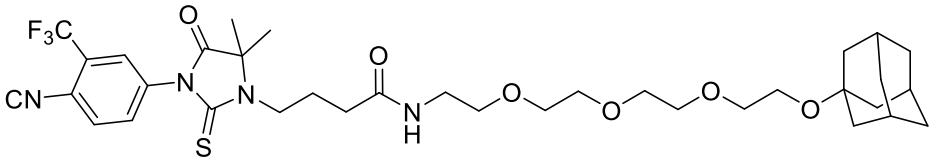

Figure 1.2. *An example of a SARD as published in a study by Gustafson et. Al [14].*

Our design incorporated derivatives of the well-established non-steroidal antiandrogens enzalutamide (Figure 1.3B) [28] and RU59063 [39, 40] conjugated to genistein via an alkyl or PEG linker (Figure 1.3C). We hypothesize that the hydrophobicity of the genistein moiety would emulate a hydrophobic tag conjugated to an antiandrogen which would allow for the selective binding to AR protein and subsequent degradation by the UPS. Furthermore, the accumulation our bifunctional compound in the prostate may allow for the beneficial regulation of several cellular pathways via the genistein moiety.

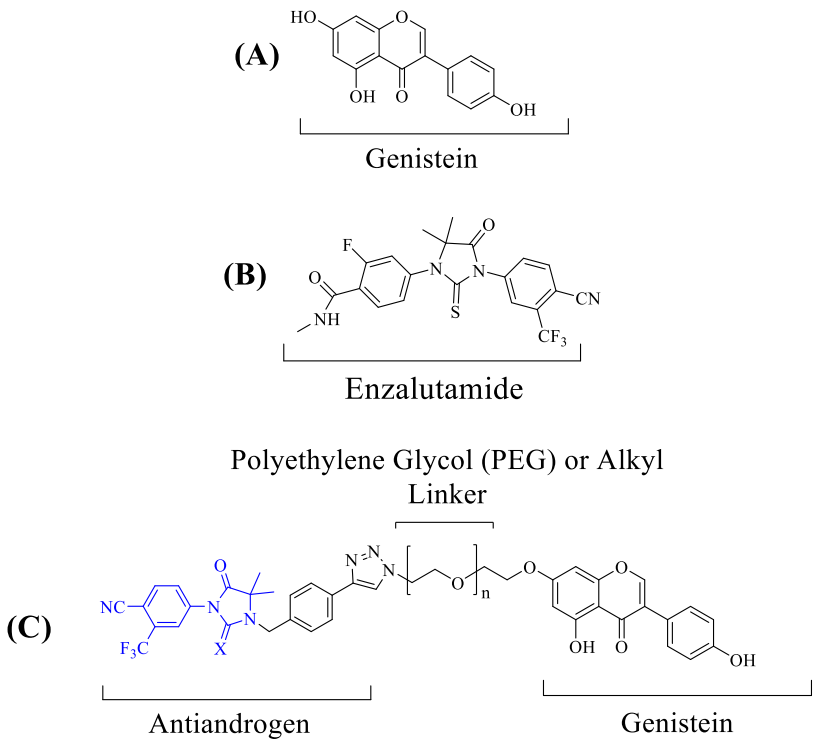

Figure 1.3 (A) *Structure of genistein,* ***(B)*** *structure of the FDA approved antiandrogen enzalutamide (Xtandi®),* ***(C)*** *Design for an enzalutamide-derived antiandrogen-genistein compound (X = Oxygen(O) or Sulfur(S)). The PEG linker length is variable to optimize the overall size of the compound.*

CHAPTER 2

METHODOLOGY

I. SYNTHESIS

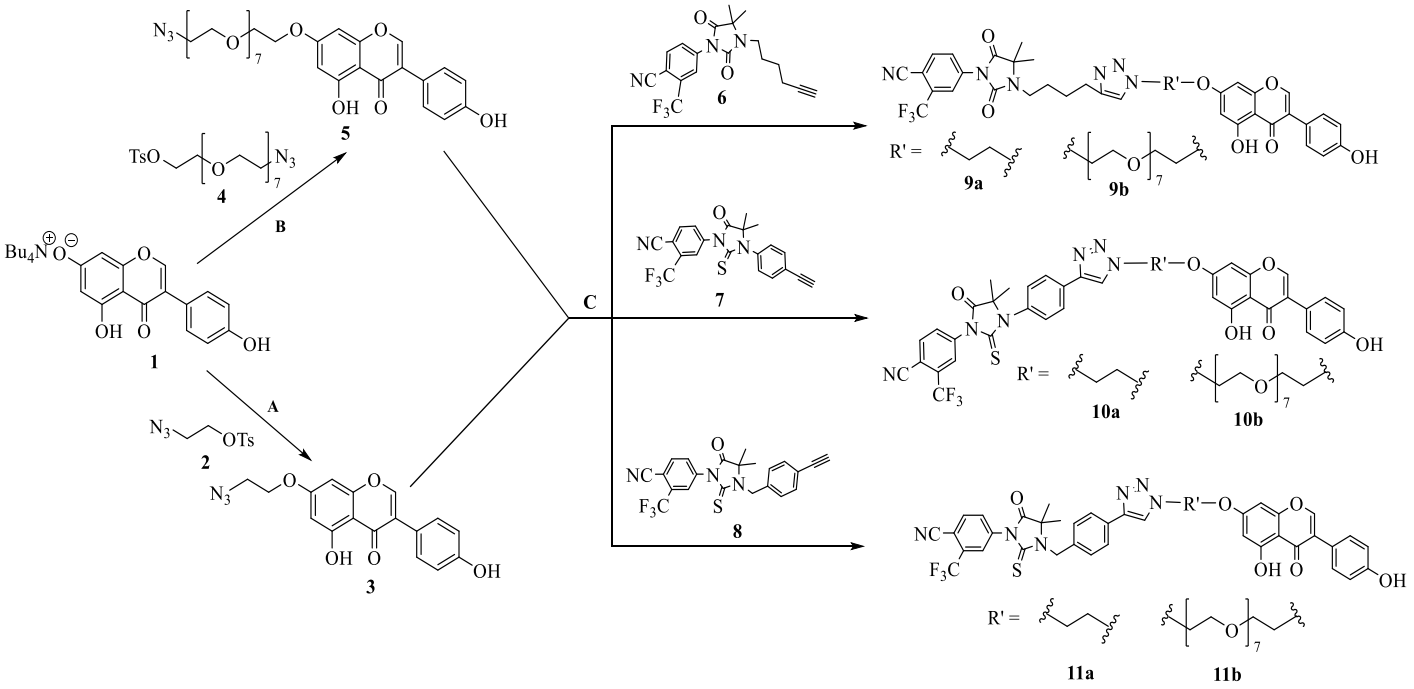

Reagents and Conditions: ***(A)*** DMF at 100^{o}C for 12h ***(B)*** KI in DMF at 100^{o}C for 12h***(C)*** CuI, DIPEA, in DMSO at RT for 2h.

Figure 2.1 *Synthetic scheme for target compounds.*

The tetrabutylammonium salt of genistein (**1**), 2-azidoethyl 4-methylbenzenesulfonate **(2)**, and PEG-Tosyl-Azide **(4)** were prepared as previously reported in the literature [41-43]. Variable linker lengths were employed to test the effects of a short alkyl linker compared to a long, flexible PEG linker. Genistein-alkyl-azide **(3)** and genistein-PEG-azide **(5)** were made via the condensation of **(1)** with **(2)** and **(4),** respectively. Subsequent Cu(I) catalyzed Huisgen cycloaddition reactions [44] between the azides **(3** and **5)** and the terminal alkynes on **6, 7,** and **8** yielded the desired conjugates: **9a-b**, **10a-b**, and **11a-b.**

II. CELL CULTURE AND MATERIALS

LNCaP and DU145 cells were obtained from ATCC (Manassas, VA). MCF-7 was a gift from Dr. Al Merrill's laboratory (Georgia Institute of Technology, Atlanta, GA). Cells were routinely cultured in phenol-red free RPMI-1640 (Lonza, Walkersville, MD) for LNCaP, EMEM (Quality Biological, Gaithersburg, MD) for DU145, and DMEM (Corning, Manassas, VA) for MCF-7 as per the manufacturer's suggested protocols with 10% fetal bovine serum (FBS) (Atlanta Biologicals, Norcross, GA) and Penicillin/Streptomycin (Sigma-Aldrich, St. Louis, MO). All cell cultures were incubated at 37 °C under a 5% CO_2 atmosphere. The following antibodies were used in immunoblotting studies: AR (Sigma-Aldrich, St. Louis, MO), actin (Cell Signaling Technologies, Danvers, MA). Propidium iodide (Calbiochem-Millipore, Darmstadt, Germany) was used in cell cycle experiments, and Bortezomib (gift from Ronghu Wu's lab, Georgia Institute of Technology, Atlanta, GA) was used as a protease inhibitor in immunoblotting in addition to RNAse inhibitor (Amresco, Solon, OH). DMSO (Sigma-Aldrich, St. Louis, MO), enzalutamide (Cayman Chemical, Ann Arbor, MI), and genistein (TCI America, Portland, OR) were used in multiple assays.

Cell Lines

1. LNCaP– an androgen dependent prostate cancer cell line
2. DU145 – an androgen independent prostate cancer cell line
3. MCF-7 – a hormone (estrogen) sensitive breast cancer cell line

III. CELL VIABILITY ASSAY

For all experiments, cells (4,500 cells per well) were grown in 96-well cell culture treated microtiter plates (Sigma-Aldrich, St. Louis, MO) with the appropriate compound in triplicate for 72 h. An MTS assay (CellTiter 96 Aqueous One Solution, Promega, Madison, WI) was used to determine cell viability following manufacturer instructions. Logit plot

analysis in GraphPad Prism (GraphPad Software, La Jolla, CA) was used to determine IC_{50} values.

IV. WESTERN BLOT ANALYSIS

LNCaP cells (10^6 cells/dish) were seeded in petri dishes 24 hour prior to treatment with various concentrations of compounds for 24h. For the UPS inhibition study, cells were incubated with Bortezomib, a protease inhibitor, at 20 nM and 40 nM for 2 hours, prior to treatment with the target compounds. Thereafter, media was removed and cells were washed with chilled 1X PBS buffer and resuspended in CelLyticM buffer containing a cocktail of protease inhibitor (Sigma-Aldrich, St. Louis, MO, USA). Protein concentration was determined through Bradford protein assay. Equal amount of protein was then loaded onto an SDS-page gel (Bio-Rad, Hercules, CA, USA) and resolved by electrophoresis at a constant voltage of 100 V for 2 h. The gel was transfered onto a nitrocellulose membrane and probed for AR, and actin as loading control.

V. CELL CYCLE ANALYSIS

LNCaP cells were seeded onto 6-well plates at a density of 1×10^6 cells in 5 mL of media, and incubated in a humidified 5% CO_2 atmosphere at 37 °C overnight. Following aspiration of media, fresh media containing drugs were added to the cells and incubated for 24 h. After incubation, cells were trypsinized, harvested and fixed with 70% EtOH. Fixed cells were stained with freshly prepared propidium iodide solution containing RNAse A, and then analyzed on flow cytometer (BD FACS Acuri, BD Bioscience, San Jose, CA, USA). Unstained cells were used as control. Each experiment was performed in triplicate.

CHAPTER 3

RESULTS

ACKNOWLEDGEMENT:

I would like to sincerely thank Idris Raji for his significant contributions and mentorship in the cell and molecular biology components of this project.

I. SYNTHESIS

All target compounds were successfully synthesized. ^{1}H NMR spectra, ^{13}C NMR spectra, and mass spectroscopy data can be found in appendices B and C respectively. Detailed synthetic methods are also included in appendix A.

II. CONJUGATE 9B SIGNIFICANTLY REDUCES CANCER CELL VIABILITY

The antiproliferative potential of the synthesized compounds were evaluated in both androgen dependent (LNCaP) and androgen independent (DU145) PCa cells as well as in breast cancer cells (MCF-7). A preliminary screen of our compounds in LNCaP and DU145 identified conjugate **9b** as our lead (data not shown). In LNCaP, genistein exhibited an IC_{50} of 24.02 ± 0.9 µM (Figure 3.1). A combination of enzalutamide and genistein did not significantly improve upon the IC_{50} obtained by genistein, however our lead conjugate (**9b)**, exhibited micromolar inhibition of LNCaP with an IC_{50} of 1.44 ± 0.9 µM (Figure 3.2).

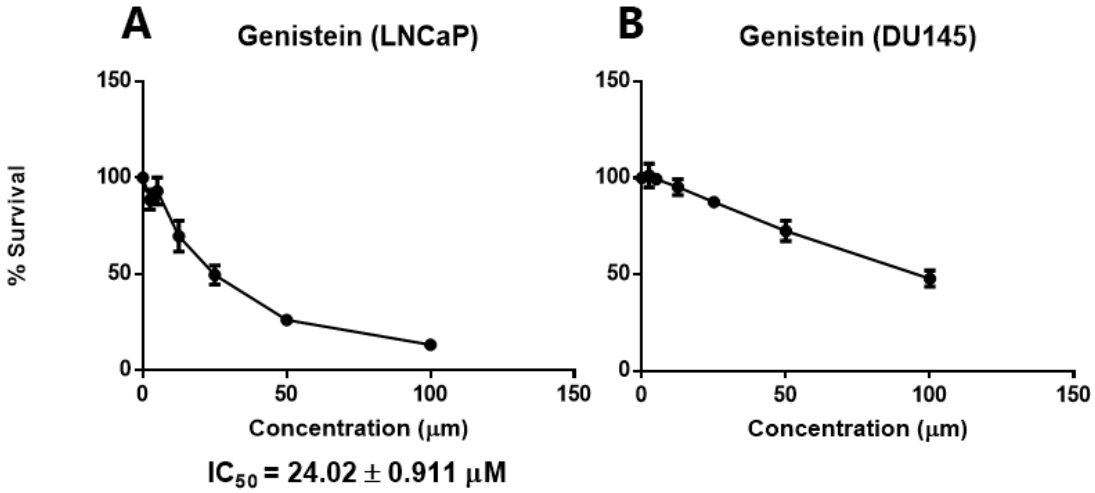

Figure 3.1 (A) *Dose response curve for genistein in LNCaP.* ***(B)*** *Dose response curve for genistein in DU145.*

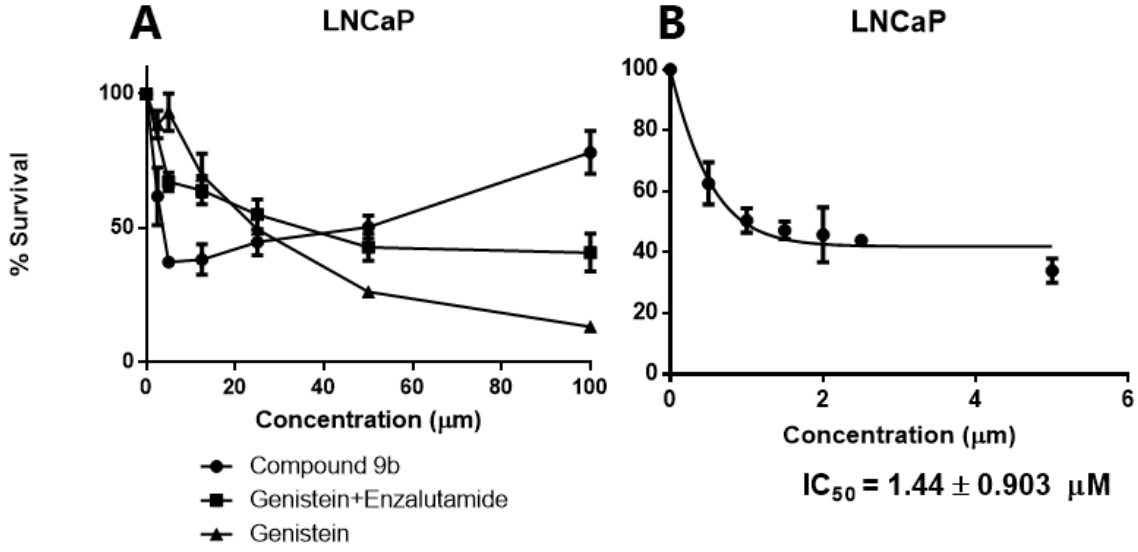

Figure 3.2 (A) *Dose response curve for genistein, genistein and enzalutamide, and* ***9b*** *in LNCaP.* ***(B)*** *Dose response curve for conjugate 9b at lower concentrations in LNCaP with fit line to determine* IC_{50}.

In DU145, conjugate **9b** exhibited an IC_{50} of 3.38 ± 0.9 µM (Figure 3.3). In comparison to a combination of enzalutamide and genistein (IC_{50} = 31.71 ± 0.8) in LNCaP cells as given by Figure 3.4, **9b** is significantly more active. The combination of enzalutamide and genistein in DU145 cells resulted in dose-dependent activity, however 50% inhibition was not obtained in the tested concentration range and IC_{50} values were not able to be calculated.

With higher concentrations (> 20 µM), **9b** was observed to aggregate and precipitate out of the culture media in both LNCaP and DU145. As such, a higher survival percentage was observed at these concentrations in both cell lines (Figures 3.2 and 3.3). A similar pattern in cellular toxicity was observed in MCF-7 cells (Figure 3.5), which served as a model of hormone-responsive (estrogen) breast cancer.

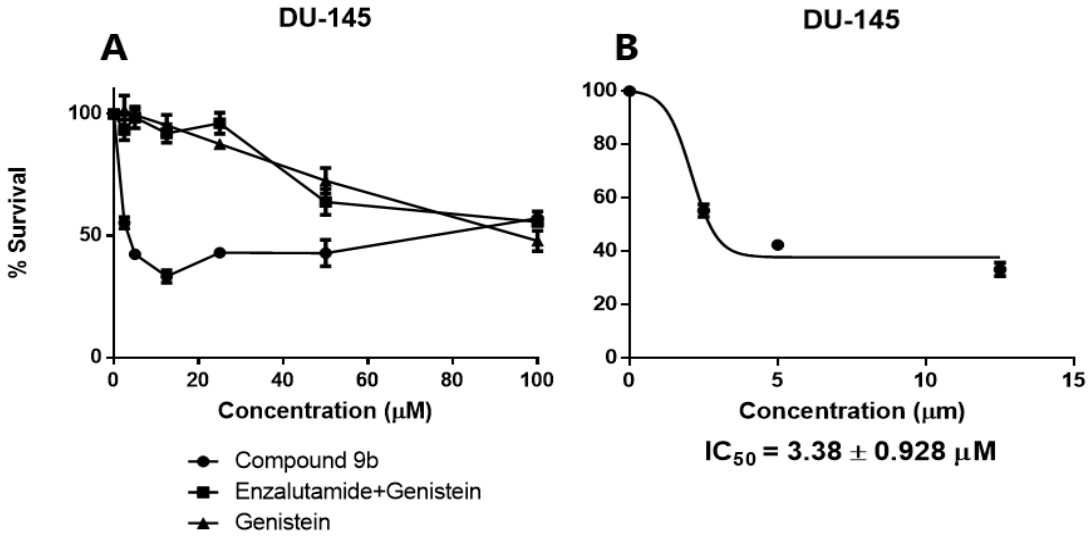

Figure 3.3 (A) *Dose response curves for genistein, genistein + enzalutamide, and* ***9b*** *in DU145.* ***(B)*** *Dose response curve for conjugate 9b at lower concentrations in DU145 with fit line to determine* IC_{50}.

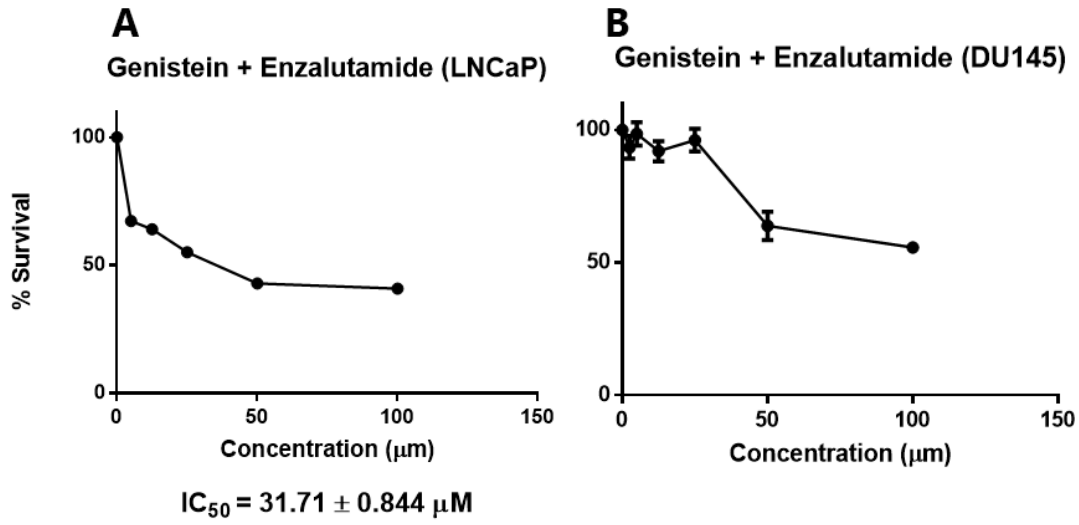

Figure 3.4 *Dose responsive curves for a combination of genistein and enzalutamide (equimolar concentrations at each point) in* ***(A)*** *LNCaP and* ***(B)*** *DU145.*

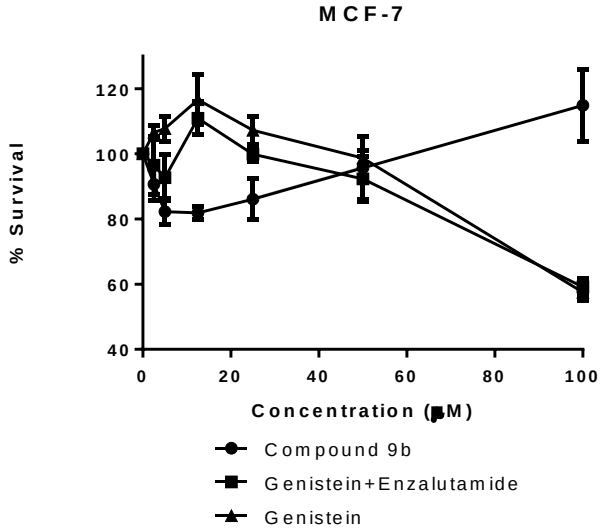

Figure 3.5 *Dose responsive curves for a combination of genistein and enzalutamide in the breast cancer cell line MCF-7.*

III. CONJUGATE 9B DEGRADES ANDROGEN RECEPTOR IN A DOSE-DEPENDENT MANNER

The dose dependent degradation of androgen receptor is observed from the data given in Figure 3.6. As exhibited by lanes 2-4, the expression of AR decreases as the concentration of conjugate **9b** increases from 0.5 μM to 2.5 μM. With the incubation of a high concentration (40 μM) of the non-steroidal antiandrogen alkyne component of compound **9b** (compound **6**) in lane 5, the expression of AR was found to be greater than that of in lane 4 where cells were treated with 2.5 μM of compound **9b**.

To preliminary examine if UPS inhibition could rescue AR degradation, we incubated cells with various concentrations of compound **9b** and the proteasome inhibitor Bortezomib (lanes 7-9). A comparison between lanes 7 and 8 shows that the same concentration of a proteasome inhibitor has a smaller effect (lane 8) on re-expressing AR with higher concentrations of compound **9b**. The results from lane 9 may be interpreted to indicate that a higher concentration of Bortezomib is able to further rescue AR expression (in comparison to lane 7), showing that the degradation of AR was likely mediated by the ubiquitin protease system. The comparisons in lanes 7-9, however, are not very clear due to the quality of the western blot image (Figure 3.6). Therefore, a repeat of this experiment with more concentrations of UPS inhibitor and conjugate **9b** must be carried out to validate the role of the UPS in the degradation of AR.

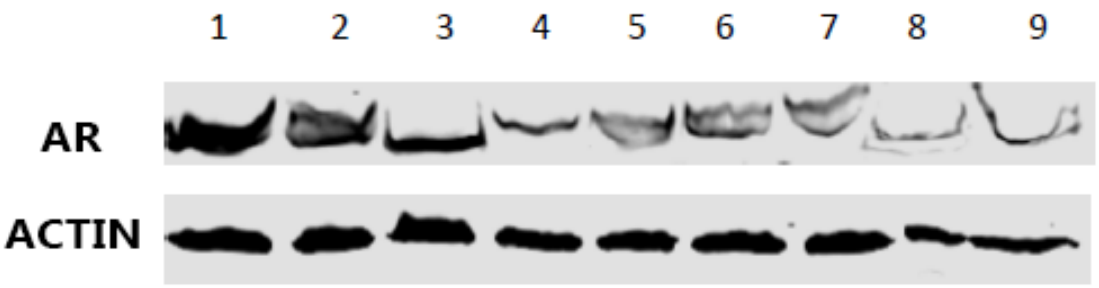

Figure 3.6 *Western blot for AR Expression. Lane 1 = DMSO, Lane 2 =* ***9b*** *(0.5 µM), Lane 3 =* ***9b*** *(1.25 µM), Lane 4 =* ***9b*** *(2.5 µM), Lane 5 = Compound 6 (40 µM), Lane 6 = Genistein (25 µM), Lane 7 =* ***9b*** *(1.25 µM) + Bortezomib (20 nM, 2 HR incubation), Lane 8 =* ***9b*** *(2.5 µM) + Bortezomib (20 nM, 2 HR inclubation), Lane 9 =* ***9b*** *(1.25 µM) + Bortezomib (40 nM, 2 HR incubation).*

IV. COMPOUND 9B INDUCES S-PHASE CELL CYCLE ARREST

Figure 3.7 shows that treatment with compound **9b** results in the shift of the cell population percentages to the S phase. Similar profiles were observed regardless of the concentration of the lead conjugate in comparison to the DMSO control. Genistein and treatment with compound **6** produce similar profiles which also indicated S phase arrest.

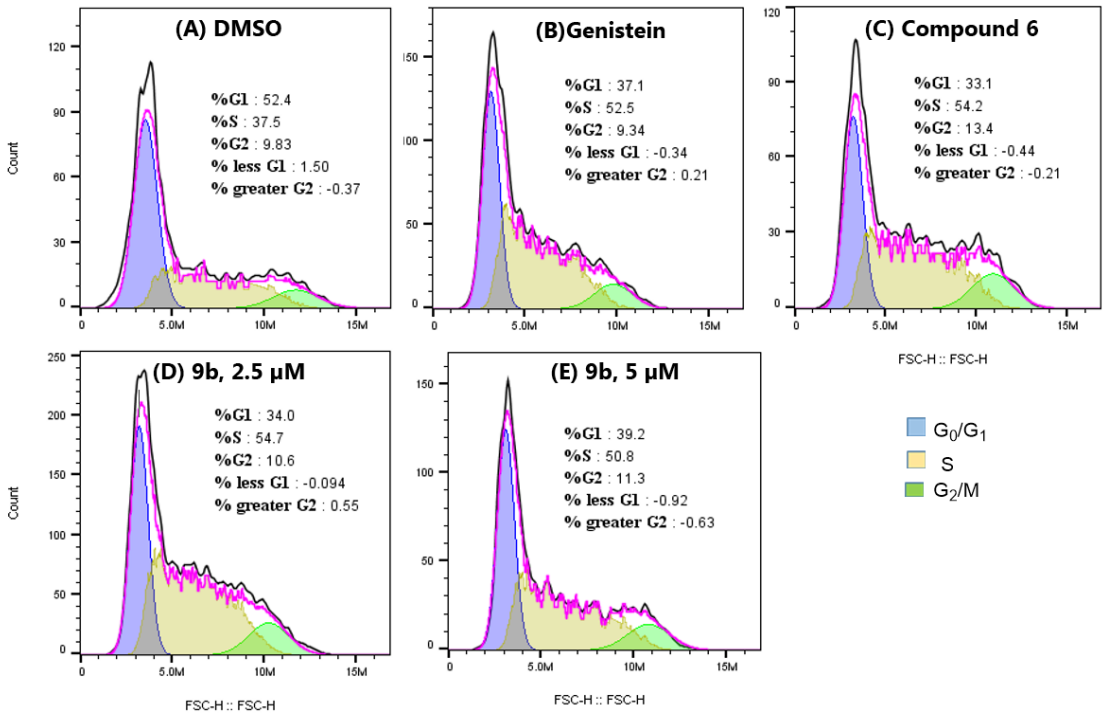

Figure 3.7 *Cell cycle profiles for LNCaP cells after treatment with* ***(A)*** *DMSO [Control],* ***(B)*** *genistein (25 µM),* ***(C)*** *compound 6 (40 µM),* ***(D,E)*** *compound 9b at 2.5 µM and 5 µM, respectively.*

CHAPTER 4

DISCUSSION

I. CONJUGATE 9B SIGNIFICANTLY REDUCES CANCER CELL VIABILITY

Conjugate **9b** was identified as the lead compound in this study after a preliminary screen of all the synthesized compounds in PCa cell lines (LNCaP and DU145). While all the PEG linker compounds (compounds **9b**, **10b**, and **11b**) exhibit inhibition of cell growth in the viability assay for both cell lines (data not shown), conjugate **9b** (Figures 3.2 and 3.3) is by far the most potent of the three and was therefore the focus of the remainder of the study.

The inhibition profile obtained for genistein (IC_{50} = 24.02 ± 0.9 µM) in LNCaP is within the range of IC_{50} values (10 µM to 40 µM) reported in the literature [45, 46]. Treatment of genistein in DU145 cells exhibits an inhibitory profile, however an IC_{50} value was not able to be calculated with the tested concentration range. In comparison to the results obtained from genistein in LNCaP cells, compound **9b** is significantly more potent. However, at higher concentrations (> 20 µM), the target compound (**9b**) began to precipitate out of the cell media in both LNCaP and DU145 cells (Figure 3.2 and 3.3). Since this phenomenon was observed, the cell viability assay was repeated with compound **9b** at lower concentrations (up to 15 µM) to calculate IC_{50} values.

With a combination of genistein and the FDA approved drug enzalutamide, an effective IC_{50} value of 31.71 ± 0.8 µM was calculated in LNCaP with equimolar concentrations of both compounds at every treatment (Figure 3.4). The combinatorial treatment of genistein and enzalutamide in DU145 cells exhibits an inhibitory profile, however an IC_{50} value was not able to be calculated with the tested concentration range (Figure 3.4). In comparison to genistein alone, a combination of an antiandrogen and genistein exhibits less potent inhibition as indicated by a higher IC_{50} value. However, the conjugation of a non-steroidal antiandrogen (an enzalutamide derivative) and genistein

via a PEG linker as given by compound **9b** significantly outperforms a combinatorial treatment of the two agents as separate molecules.

The effects of genistein, genistein + enzalutamide, and compound **9b** were evaluated in estrogen sensitive MCF-7 breast cancer cells to evaluate the effect of the target compounds in other hormone-receptor driven cancers (Figure 3.5). This study was also done to characterize whether the initial estrogenic effects of genistein that stimulate breast cancer growth [47] could be observed in the target compounds. Incubation with genistein as well as combinatorial treatment with enzalutamide is found to initially increase cancer cell growth, followed by inhibition at higher concentrations (> 20 μM)shown in Figure 3.5. In contrast, treatment with compound **9b** at lower concentrations (up to 15 μM) inhibits cancer cell growth. As with LNCaP and DU145, the conjugate precipitates out of the cell culture media at higher concentrations (> 20 μM). Since agonistic behavior is not observed with the lead compound (Figure 3.5), the incorporation of the genistein moiety on a bifunctional molecule may reduce the estrogenic potential of the group.

The selective toxicity of compound **9b** was evaluated by comparing the calculated IC_{50} values between LNCaP, an androgen sensitive PCa cell line, and DU145, an androgen insensitive PCa cell line representative of CRPC. A lower IC_{50} value in LNCaP (1.44 ± 0.9 μM) in comparison to DU145 (3.37 ± 0.9 μM) indicates that compound **9b** is more potent in LNCaP compared to DU145. As such, selective toxicity is observed in which androgen sensitive PCa cells are more responsive to treatment in comparison to androgen insensitive cells.

The results of the cell viability assay in PCa cells suggest a link between AR expression and drug efficacy for the lead conjugate. As such, the effect of the lead compound on the expression of androgen receptor was evaluated via western immunoblotting with a protocol adapted from Gustafson and colleagues [14].

II. CONJUGATE 9B DEGRADES ANDROGEN RECEPTOR IN A DOSE-DEPENDENT MANNER

As shown in Figure 3.6, the dose-dependent degradation of androgen receptor is observed with increasing concentrations of conjugate **9b**. The secondary component of this study sought to link the degradation of AR to the ubiquitin protease system. The incubation of LNCaP cells with Bortezomib, a UPS inhibitor should theoretically rescue AR expression if UPS mediated degradation is the primary means of downregulation in the cells. However, the results from the western blot were not clear enough to be conclusive. Nevertheless, this data may be interpreted as a preliminary study that shows the strong possibility that the observed AR degradation could be UPS mediated. Further studies are currently planned in the future to generate a clearer western blot image by varying the concentration range of the target compound and test other UPS inhibitors such as epoxomycin.

III. COMPOUND 9B INDUCES S-PHASE CELL CYCLE ARREST

The results of the cell cycle study (Figure 3.7) indicate that the target compound induces S-phase arrest in comparison to the control. While these results also indicate that genistein also induces S-phase arrest, several sources in the literature report that G_2/M and G_1 arrest was the primary mode of cell cycle arrest in LNCaP (and other) cells incubated with genistein [46, 48, 49]. Since the experimental results of this study are in conflict with those reported in the literature, a follow up study of this assay must be performed to confirm that S-phase arrest is indeed occurring in LNCaP cells treated with genistein and the target compounds.

IV. CONCLUSIONS

This study explored the efficacy of a bifunctional molecule; specifically a combination of a potent antiandrogen and genistein on the growth of various prostate and breast cancer cells as well as the extent of UPS mediated AR degradation. Preliminary cell viability studies have identified a promising lead compound (compound **9b**) within the synthesized conjugates. This compound exhibits potent inhibition of cell growth in androgen insensitive LNCaP cells (IC_{50} = 1.44 ± 0.9 μM), androgen insensitive DU145 cells (IC_{50} = 3.38 ± 0.9 μM). Western immunoblotting studies confirmed the dose-dependent degradation of AR and cell cycle analyses indicate S-phase arrest with the treatment of compound **9b**. While preliminary immunoblotting studies suggest the degradation of AR is mediated by the ubiquitin protease system (UPS), further studies must be carried out to validate these preliminary results.

V. FUTURE DIRECTIONS

As mentioned previously in the discussion, western immunoblotting studies will need to be repeated with various concentrations of conjugate **9b** as well as the incorporation of other UPS inhibitors such as epoxomycin. The cell cycle study must also be repeated to confirm whether the observed results truly conflict with the established literature for the effect of genistein on LNCaP cells. In addition to these required studies, androgen receptor binding studies will also need to be carried out on all the synthesized target compounds to characterize the effect of adding the genistein moiety on the binding affinity of the antiandrogen to AR. Matrigel invasion chamber assays may also be performed to study the effect of the target compounds on the metastatic potential of PC3 PCa cells.

APPENDIX A

SUPPLEMENTARY INFORMATION

I. SYNTHETIC PROTOCOLS

***Synthesis of 7-(2-azidoethoxy)-5-hydroxy-3-(4-hydroxyphenyl)-4H-chromen-4-one* (3)**

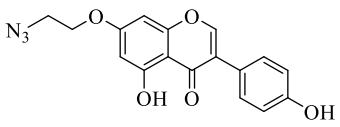

1 (0.5 g, 0.9 mmol) and **2** (0.56 g, 2.33 mmol) were dissolved in DMF (25 mL). The mixture was reacted overnight at 50° C. The product was purified via column chromatography 5% Acetone: 95% DCM. The product was yielded as a white solid. (232.5 mg, 70.2 %). 1H NMR (400 MHz, dmso) δ 12.97 (d, J = 6.3 Hz, 1H), 9.64 (s, 1H), 8.42 (s, 1H), 7.48 – 7.33 (m, 2H), 6.90 – 6.79 (m, 2H), 6.69 (d, J = 2.3 Hz, 1H), 6.42 (d, J = 2.3 Hz, 1H), 4.34 – 4.25 (m, 2H), 3.74 – 3.66 (m, 2H). MS (ESI) *m/z* calculated $C_{17}H_{13}O_5N_3$ [M+H$^+$]: 339.09, found 339.17.

***Synthesis of 7-((23-azido-3,6,9,12,15,18,21-heptaoxatricosyl)oxy)-5-hydroxy-3-(4-hydroxyphenyl)-4H-chromen-4-one* (5).**

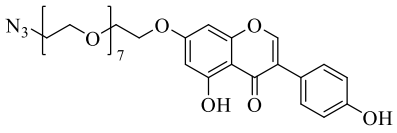

1 (0.270 g, 0.525 mmol), **4** (0.318 g, 0.575 mmol) and KI (0.01 g, 0.05 mmol) were dissolved in 5 mL of DMF. The mixture was reacted overnight at 100° C. The product was purified via preparative TLC (1:3 Acetone/DCM and eluent: 2:3 Acetone/DCM). The product was obtained as a pale yellow oil. (330 mg, 96.9 %). ^{1}H NMR (400 MHz, cdcl$_3$) δ 12.83 (s, 1H), 8.01 (s, 1H), 7.77 (s, 1H), 7.38 – 7.30 (m, 2H), 6.92 – 6.85 (m, 2H), 6.32 (q, *J* = 2.3 Hz, 2H), 4.11 – 4.03 (m, 2H), 3.87 – 3.81 (m, 2H), 3.74 – 3.67 (m, 4H), 3.67 – 3.62 (m, 22H), 3.40 – 3.34 (m, 2H). HRMS (ESI) *m/z* calculated for $C_{39}H_{30}O_6N_6F_3S$ [M+H$^+$]: 670.2572, found 670.2566.

Synthesis of 4-(3-(4-(1-(2-((5-hydroxy-3-(4-hydroxyphenyl)-4-oxo-4H-chromen-7-yl)oxy)ethyl)-1H-1,2,3-triazol-4-yl)butyl)-4,4-dimethyl-2,5-dioxoimidazolidin-1-yl)-2-(trifluoromethyl)benzonitrile **(9a)**

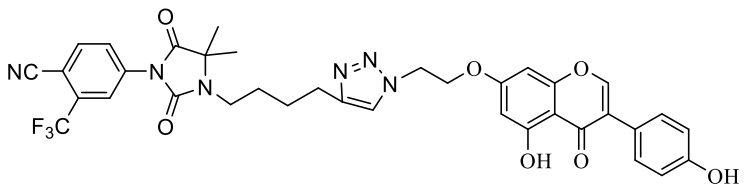

Chemical Formula: $C_{36}H_{31}F_3N_6O_7$
Molecular Weight: 716.67

6 (100 mg, 0.26 mmol), **3** (89.9 mg, 0.26 mmol), and DIPEA (59.93 mg, 0.46 mmol) were dissolved in anhydrous DMSO under argon. Copper (I) Iodide (25.23 mg, 0.13 mmol) was added and the reaction mixture was stirred under argon at ambient temperature overnight. The reaction was diluted with DCM and washed with 1:4 NH_4OH/Saturated NH_4Cl (3x30 mL) and saturated NH_4Cl (30 mL) and the organic layer was dried under sodium sulfate, filtered and concentrated in vacuo. Column chromatography (eluent 80:4:1 – DCM: Acetone: MeOH) gave the product as an orange-white solid. (105.3 mg, 56 %). ^{1}H NMR (400 MHz, dmso) δ 12.93 (s, 1H), 9.61 (s, 1H), 8.28 (d, *J* = 8.4 Hz, 1H), 8.17 (d, *J* = 2.0 Hz, 1H), 8.01 (dd, *J* = 8.4, 1.6 Hz, 1H), 7.94 (s, 1H), 7.42 – 7.33 (m, 2H), 6.85 – 6.77 (m, 2H), 6.65 (d, *J* = 2.3 Hz, 1H), 6.38 (d, *J* = 2.3 Hz, 1H), 4.74 (t, *J* = 4.9 Hz, 2H), 4.51 (t, *J* = 4.9 Hz, 2H), 3.33 (s, 6H), 2.67 (s, 2H), 1.64 (s, 5H), 1.41 (s, 7H). ^{13}C NMR (101 MHz, dmso) δ 180.9, 175.1, 164.1, 162.2, 157.9, 157.8, 155.0, 152.9, 147.1, 136.5, 130.7, 130.4, 123.0, 115.5, 106.1, 98.9, 93.4, 67.5, 62.0, 31.2, 28.8, 26.7, 25.0, 22.9. HRMS (ESI) *m/z* calculated for $C_{36}H_{32}O_7N_6F_3$ [M+H$^+$]: 717.2275, found 717.2279.

Synthesis o 4-(3-(4-(1-(2-((5-hydroxy-3-(4-hydroxyphenyl)-4-oxo-4H-chromen-7-yl)oxy)ethyl)-1H-1,2,3-triazol-4-yl)phenyl)-4,4-dimethyl-5-oxo-2-thioxoimidazolidin-1-yl)-2-(trifluoromethyl)benzonitrilef **(10a)**

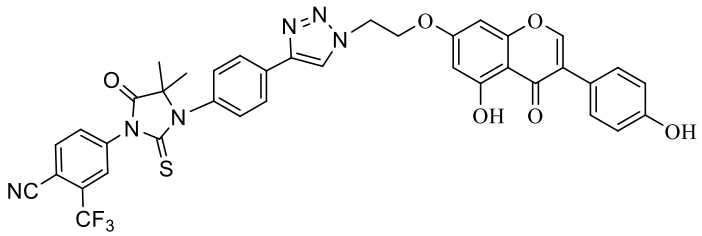

Chemical Formula: $C_{38}H_{27}F_3N_6O_6S$
Molecular Weight: 752.73

7 (121 mg, 1 mmol), **3** (100 mg, 1 mmol), and DIPEA (66 mg, 1.75 mmol) were dissolved in anhydrous DMSO under argon. Copper (I) Iodide (28 mg, 0.5 mmol) was added and the reaction mixture was stirred under argon at ambient temperature overnight. The reaction was diluted with DCM and washed with 1:4 NH_4OH/Saturated NH_4Cl (3x30 mL) and saturated NH_4Cl (30 mL) and the organic layer was dried under sodium sulfate, filtered and concentrated in vacuo. Column chromatography (eluent 80:4:1 – DCM: Acetone: MeOH) gave the product as a white solid. (141.1 mg, 77.4%). ^{1}H NMR (400 MHz, dmso) δ 12.95 (s, 1H), 9.60 (s, 1H), 8.76 (s, 1H), 8.39 (d, *J* = 11.0 Hz, 2H), 8.31 (s, 1H), 8.09 (d, *J* = 8.3 Hz, 1H), 8.04 (d, *J* = 8.6 Hz, 2H), 7.46 (d, *J* = 8.6 Hz, 2H), 7.38 (d, *J* = 8.7 Hz, 2H), 6.81 (d, *J* = 8.8 Hz, 2H), 6.72 (d, *J* = 2.3 Hz, 1H), 6.47 (d, *J* = 2.2 Hz, 1H), 5.74 (s, 1H), 4.88 (s, 2H), 4.60 (s, 2H), 3.33 (s, 6H). ^{13}C NMR (101 MHz, dmso) δ 180.9, 180.4, 175.5, 164.1, 162.3, 157.9, 146.1, 138.6, 136.6, 135.2, 134.5, 132.0, 130.9, 130.6, 126.7, 123.2, 123.0, 121.5, 115.5, 106.2, 105.0, 93.5, 66.9, 60.2, 31.2, 23.4. HRMS (ESI) *m/z* calculated for $C_{38}H_{28}O_6N_6F_3S$ [M+H$^+$]: 753.1714, found 753.1738.

Synthesis of 4-(3-(4-(1-(2-((5-hydroxy-3-(4-hydroxyphenyl)-4-oxo-4H-chromen-7-yl)oxy)ethyl)-1H-1,2,3-triazol-4-yl)benzyl)-4,4-dimethyl-5-oxo-2-thioxoimidazolidin-1-yl)-2-(trifluoromethyl)benzonitrile **(11a)**

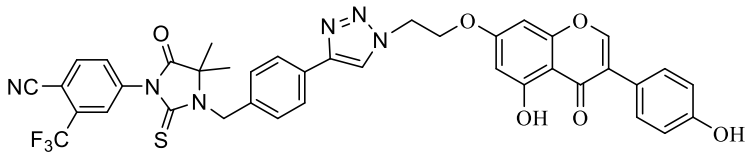

Chemical Formula: $C_{39}H_{29}F_3N_6O_6S$
Molecular Weight: 766.75

8 (25 mg, 0.06 mmol), **3** (19.86 mg, 0.06 mmol), and DIPEA (12.9 mg, 0.1 mmol) were dissolved in anhydrous DMSO under argon. Copper (I) Iodide (5.57 mg, 0.03 mmol) was added and the reaction mixture was stirred under argon at ambient temperature overnight. The reaction was diluted with DCM and washed with 1:4 NH_4OH/Saturated NH_4Cl (3x30 mL) and saturated NH_4Cl (30 mL) and the organic layer was dried under sodium sulfate, filtered and concentrated in vacuo. Column chromatography (eluent 80:4:1 – DCM: Acetone: MeOH) gave the product as a white solid. (51.5 mg, 87.1%).

1H NMR (400 MHz, dmso) δ 12.98 (s, 1H), 9.65 (s, 1H), 8.70 (s, 1H), 8.47 – 8.34 (m, 2H), 8.14 (d, J = 8.4 Hz, 1H), 7.86 (d, J = 8.2 Hz, 2H), 7.59 (d, J = 8.5 Hz, 2H), 7.41 (d, J = 8.7 Hz, 2H), 6.84 (d, J = 8.6 Hz, 2H), 6.49 (s, 1H), 5.16 (s, 2H), 4.88 (s, 2H), 4.61 (s, 2H), 3.37 (s, 16H). HRMS (ESI) *m/z* calculated for $C_{39}H_{30}O_6N_6F_3S$ $[M+H^+]$: 767.1895, found 767.1894.

Synthesis of 4-(3-(4-(1-(23-((5-hydroxy-3-(4-hydroxyphenyl)-4-oxo-4H-chromen-7-yl)oxy)-3,6,9,12,15,18,21-heptaoxatricosyl)-1H-1,2,3-triazol-4-yl)butyl)-4,4-dimethyl-2,5-dioxoimidazolidin-1-yl)-2-(trifluoromethyl)benzonitrile **(9b)**

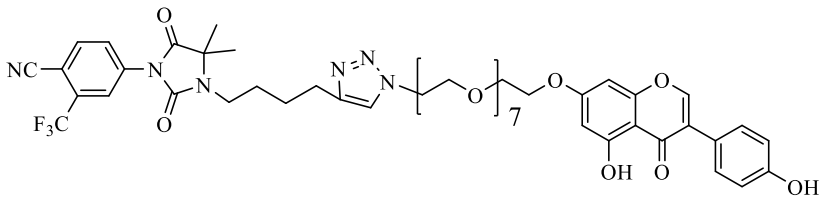

Chemical Formula: $C_{50}H_{59}F_3N_6O_{14}$
Exact Mass: 1024.40

6 (52.4 mg, 0.138 mmol), compound **5** (90 mg, 0.138 mmol), and DIPEA (31.4 mg, 0.241 mmol) were dissolved in anhydrous DMSO under argon. Copper (I) Iodide (13.2 mg, 0.07 mmol) was added and the reaction mixture was stirred under argon at ambient temperature overnight. The reaction was diluted with DCM and washed with 1:4 NH_4OH/Saturated NH_4Cl (3x30 mL) and saturated NH_4Cl (30 mL) and the organic layer was dried under sodium sulfate, filtered and concentrated in vacuo. Column chromatography (eluent 80:4:1 – DCM: Acetone: MeOH) gave the product. The product was lyophilized and gave a yellow oil. (15.2 mg, 12.8 %). ^{1}H NMR (400 MHz, $cdcl_3$) δ 12.83 (s, 1H), 8.11 (s, 1H), 7.97 (d, *J* = 10.0 Hz, 1H), 7.87 (d, *J* = 8.4 Hz, 1H), 7.78 (s, 1H), 7.52 (s, 1H), 7.31 (d, *J* = 8.5 Hz, 2H), 6.90 (d, *J* = 8.5 Hz, 2H), 6.32 (dd, *J* = 12.4, 2.2 Hz, 2H), 5.28 (s, 1H), 4.48 (s, 2H), 4.10 (s, 2H), 3.82 (s, 4H), 3.60 (t, *J* = 10.2 Hz, 23H), 3.35 (s, 2H), 2.75 (s, 2H), 2.61 (s, 2H), 1.75 (s, 4H), 1.48 (s, 5H). ^{13}C NMR (101 MHz, $cdcl_3$) δ 180.8, 174.7, 164.6, 162.5, 157.8, 157.2, 152.8, 152.6, 136.5, 135.2, 130.0, 127.9, 123.7, 122.9, 121.9, 115.7, 115.0, 106.2, 98.7, 92.9, 70.8, 70.6, 70.5, 70.4, 69.5, 69.3, 68.0, 61.9, 50.3, 40.1, 28.9, 26.8, 25.0, 23.5. HRMS (ESI) *m/z* calculated for $C_{50}H_{60}O_{14}N_6F_3$ $[M+H^+]$: 1025.4104, found 1025.4114.

Synthesis of 4-(3-(4-(1-(23-((5-hydroxy-3-(4-hydroxyphenyl)-4-oxo-4H-chromen-7-yl)oxy)-3,6,9,12,15,18,21-heptaoxatricosyl)-1H-1,2,3-triazol-4-yl)phenyl)-4,4-dimethyl-5-oxo-2-thioxoimidazolidin-1-yl)-2-(trifluoromethyl)benzonitrile **(10b).**

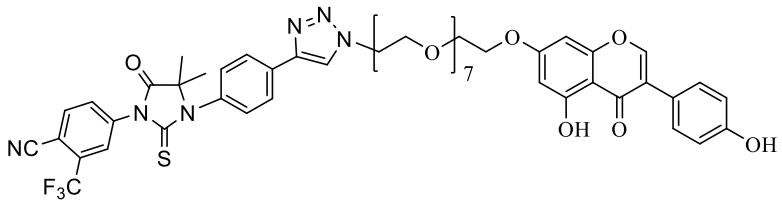

Chemical Formula: $C_{52}H_{55}F_3N_6O_{13}S$
Exact Mass: 1060.35

7 (35.8 mg, 0.086 mmol), **5** (71.2 mg, 0.11 mmol), and DIPEA (18 mg, 0.14 mmol) were dissolved in anhydrous DMSO under argon. Copper (I) Iodide (8.1 mg, 0.043 mmol) was added and the reaction mixture was stirred under argon at ambient temperature overnight. The reaction was diluted with DCM and washed with 1:4 NH_4OH/Saturated NH_4Cl (3x30 mL) and saturated NH_4Cl (30 mL) and the organic layer was dried under sodium sulfate, filtered and concentrated in vacuo. Column chromatography (eluent 80:4:1 – DCM: Acetone: MeOH) gave the product. The product was lyophilized and an orange-white solid was obtained. (28.3 mg, 30.7 %). ^{1}H NMR (400 MHz, cdcl$_3$) δ 12.83 (s, 1H), 8.12 (s, 1H), 7.99 (d, *J* = 16.0 Hz, 4H), 7.85 (d, *J* = 8.4 Hz, 1H), 7.76 (s, 1H), 7.40 – 7.29 (m, 4H), 6.90 (d, *J* = 8.5 Hz, 2H), 6.31 (d, *J* = 3.0 Hz, 2H), 4.60 (s, 2H), 4.07 (s, 2H), 3.90 (s, 2H), 3.81 (s, 2H), 3.63 (t, *J* = 20.5 Hz, 22H), 3.48 (s, 1H), 1.60 (s, 4H), 1.25 (s, 1H). ^{13}C NMR (101 MHz, cdcl$_3$) δ 179.9, 178.8, 174.0, 163.8, 161.6, 157.0, 155.9, 152.0, 145.2, 136.1, 134.4, 133.3, 132.7, 131.8, 131.6, 129.0, 125.9, 122.5, 121.4, 121.1, 119.7, 114.9, 113.7, 109.2, 105.2, 97.6, 91.9, 69.3, 68.2, 67.0, 65.6, 49.5, 22.9. HRMS (ESI) *m/z* calculated for $C_{52}H_{56}O_{13}N_6F_3S$ [M+H$^+$]: 1061.3568, found 1061.3573.

Synthesis of 4-(3-(4-(1-(23-((5-hydroxy-3-(4-hydroxyphenyl)-4-oxo-4H-chromen-7-yl)oxy)-3,6,9,12,15,18,21-heptaoxatricosyl)-1H-1,2,3-triazol-4-yl)benzyl)-4,4-dimethyl-5-oxo-2-thioxoimidazolidin-1-yl)-2-(trifluoromethyl)benzonitrile **(11b)**

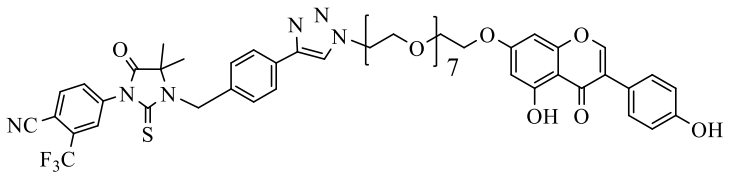

Chemical Formula: $C_{53}H_{57}F_3N_6O_{13}S$
Exact Mass: 1074.37

8 (25 mg, 0.06 mmol), compound **5** (38.5 mg, 0.06 mmol), and DIPEA (12.9 mg, 0.1 mmmol) were dissolved in anhydrous DMSO under argon. Copper (I) Iodide (5.57 mg, 0.03 mmol) was added and the reaction mixture was stirred under argon at ambient temperature overnight. The reaction was diluted with DCM and washed with 1:4 NH_4OH/Saturated NH_4Cl (3x30 mL) and saturated NH_4Cl (30 mL) and the organic layer was dried under sodium sulfate, filtered and concentrated in vacuo. Purification with preparative TLC (eluent 80:4:1 – DCM: Acetone: MeOH) gave the product. The product was lyophilized and this gave a red-orange solid. (22.1 mg, 34.3 %) ^{1}H NMR (400 MHz, cdcl$_3$) δ 12.83 (s, 1H), 8.04 (s, 1H), 8.00 – 7.92 (m, 2H), 7.83 (d, *J* = 7.9 Hz, 3H), 7.77 (s, 1H), 7.47 (d, *J* = 7.6 Hz, 2H), 7.32 (d, *J* = 8.4 Hz, 2H), 6.91 (d, *J* = 8.4 Hz, 2H), 6.32 (dd, *J* = 6.6, 2.1 Hz, 2H), 5.29 (s, 2H), 5.13 (s, 2H), 4.58 (s, 2H), 4.08 (s, 2H), 3.89 (s, 2H), 3.82 (s, 2H), 3.60 (t, *J* = 8.9 Hz, 23H), 1.46 (s, 5H), 1.24 (s, 1H). ^{13}C NMR (101 MHz, cdcl$_3$) δ 180.8, 179.9, 175.4, 164.6, 162.5, 157.8, 156.8, 152.7, 137.3, 135.9, 135.2, 132.2, 130.7, 130.1, 128.3, 127.1, 126.2, 123.2, 122.2, 115.7, 114.8, 110.0, 106.2, 98.7, 92.9, 70.8, 70.6, 70.5, 69.4, 69.3, 67.9, 65.4, 50.5, 47.3, 23.7. HRMS (MALDI) *m/z* calculated for $C_{53}H_{58}O_{13}N_6F_3S$ [M+H$^+$]: 1075.37, found 1075.3735.

APPENDIX B

^{1}H NMR AND ^{13}C NMR SPECTRA

This appendix contains ^{1}H NMR and ^{13}C NMR data from all target compounds.

^{1}H NMR (400 MHz, dmso) δ 12.93 (s, 1H), 9.61 (s, 1H), 8.28 (d, *J* = 8.4 Hz, 1H), 8.17 (d, *J* = 2.0 Hz, 1H), 8.01 (dd, *J* = 8.4, 1.6 Hz, 1H), 7.94 (s, 1H), 7.42 – 7.33 (m, 2H), 6.85 – 6.77 (m, 2H), 6.65 (d, *J* = 2.3 Hz, 1H), 6.38 (d, *J* = 2.3 Hz, 1H), 4.74 (t, *J* = 4.9 Hz, 2H), 4.51 (t, *J* = 4.9 Hz, 2H), 3.33 (s, 6H), 2.67 (s, 2H), 1.64 (s, 5H), 1.41 (s, 7H).

Appendix B - Compound 9(a) - ^{1}H NMR

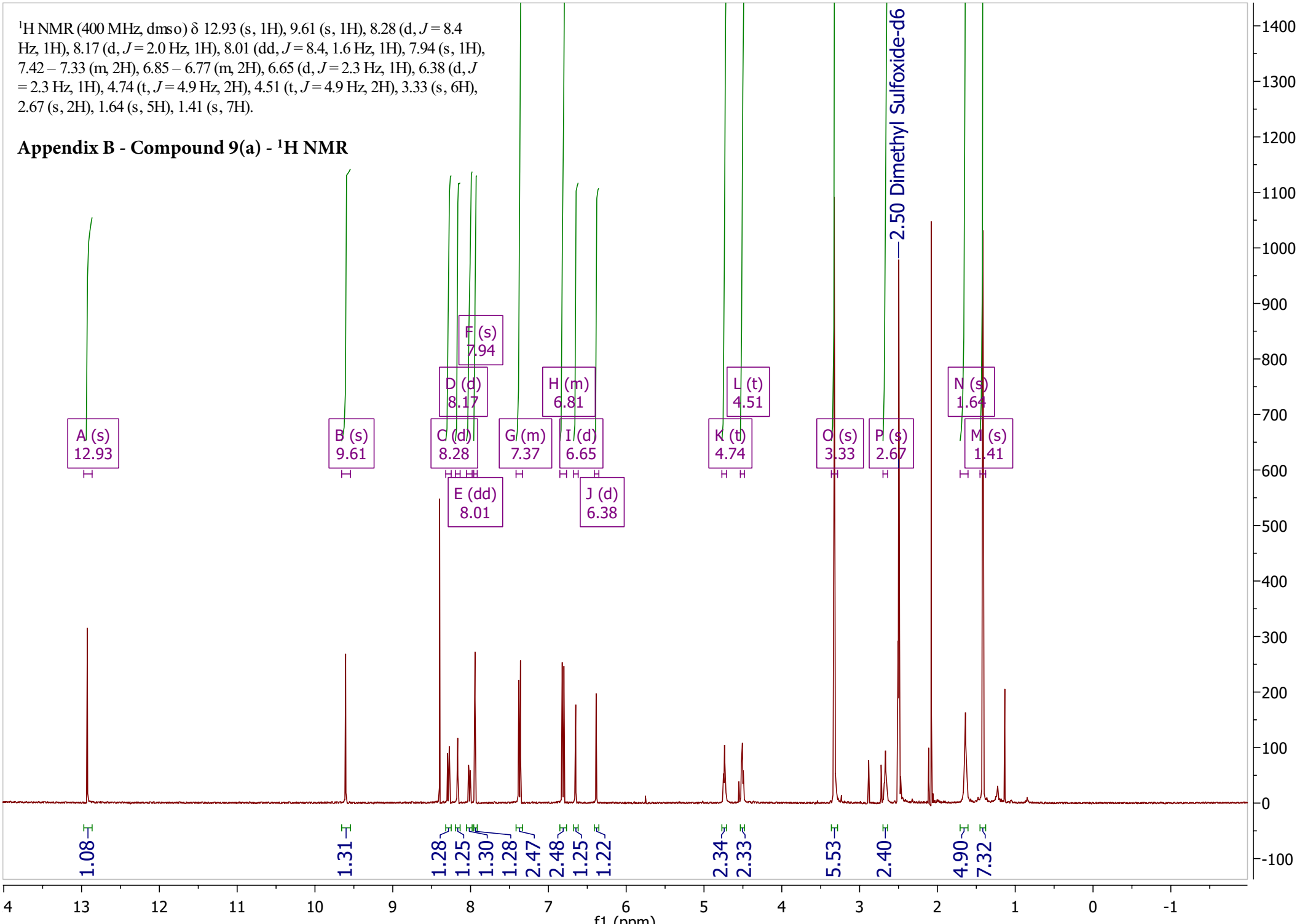

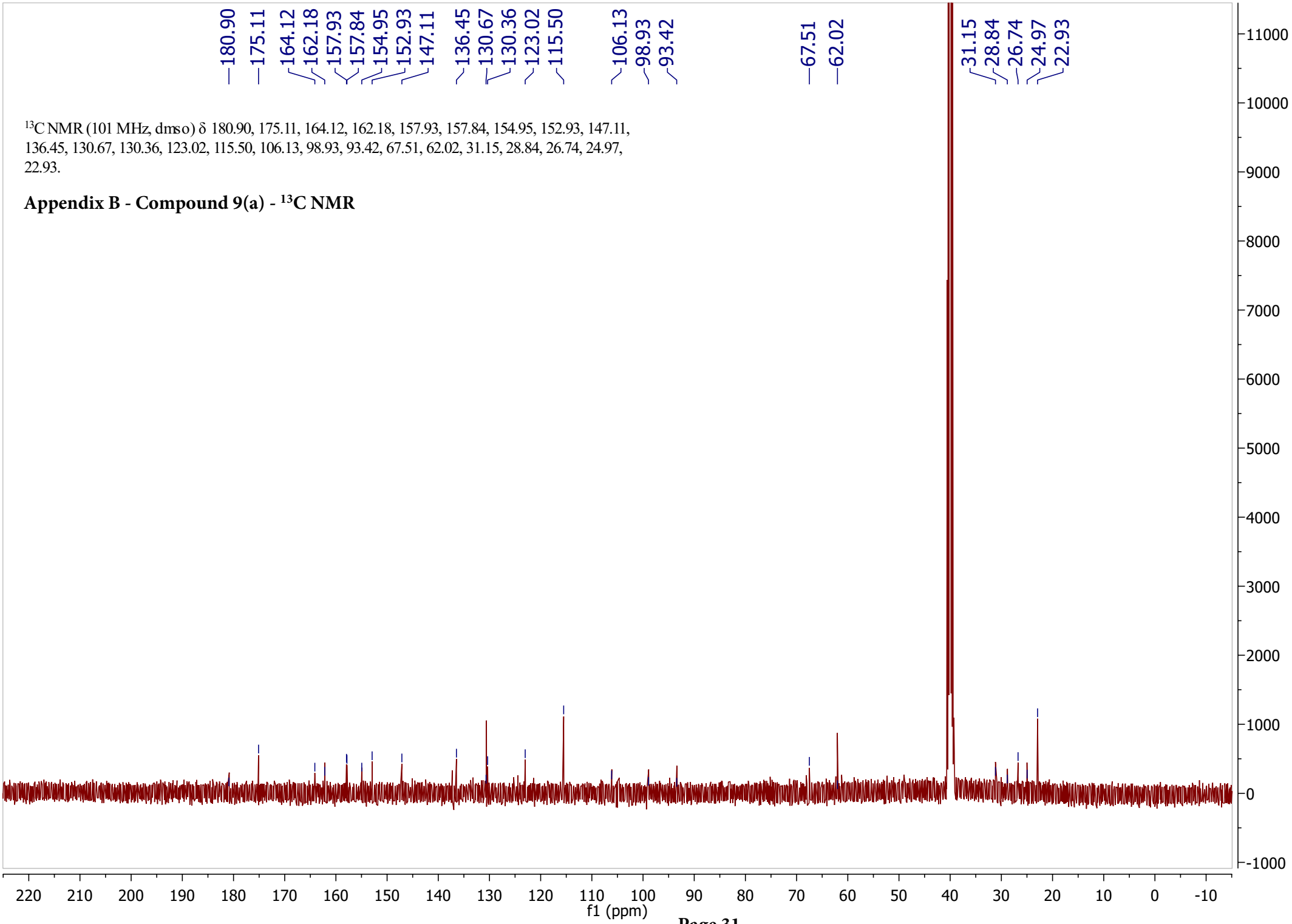

^{13}C NMR (101 MHz, dmso) δ 180.90, 175.11, 164.12, 162.18, 157.93, 157.84, 154.95, 152.93, 147.11, 136.45, 130.67, 130.36, 123.02, 115.50, 106.13, 98.93, 93.42, 67.51, 62.02, 31.15, 28.84, 26.74, 24.97, 22.93.

Appendix B - Compound 9(a) - ^{13}C NMR

^{1}H NMR (400 MHz, dmso) δ 12.95 (s, 1H), 9.60 (s, 1H), 8.76 (s, 1H), 8.39 (d, *J* = 11.0 Hz, 2H), 8.31 (s, 1H), 8.09 (d, *J* = 8.3 Hz, 1H), 8.04 (d, *J* = 8.6 Hz, 2H), 7.46 (d, *J* = 8.6 Hz, 2H), 7.38 (d, *J* = 8.7 Hz, 2H), 6.81 (d, *J* = 8.8 Hz, 2H), 6.72 (d, *J* = 2.3 Hz, 1H), 6.47 (d, *J* = 2.2 Hz, 1H), 5.74 (s, 1H), 4.88 (s, 2H), 4.60 (s, 2H), 3.33 (s, 6H).

Appendix B - Compound 10(a) - ^{1}H NMR

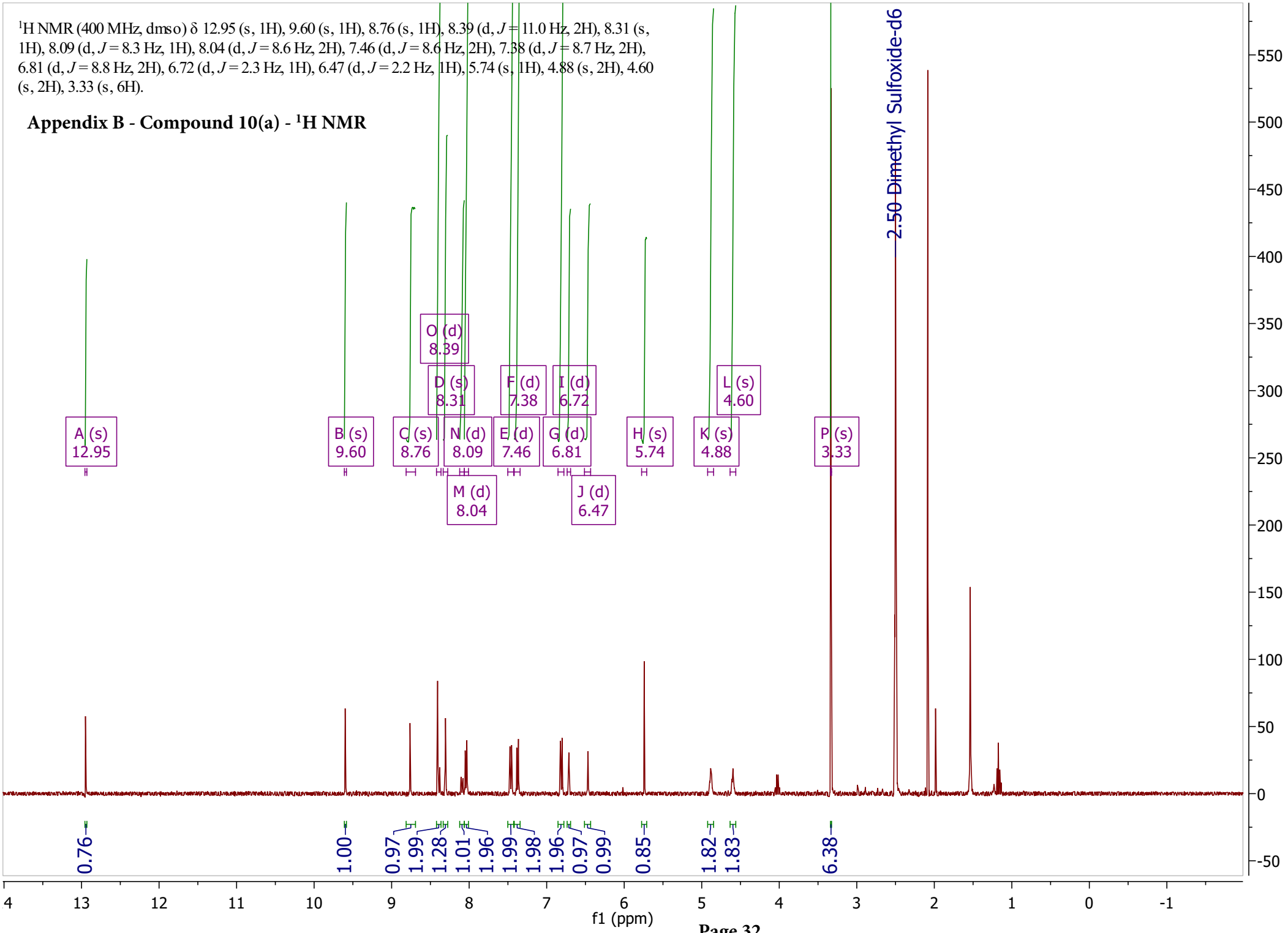

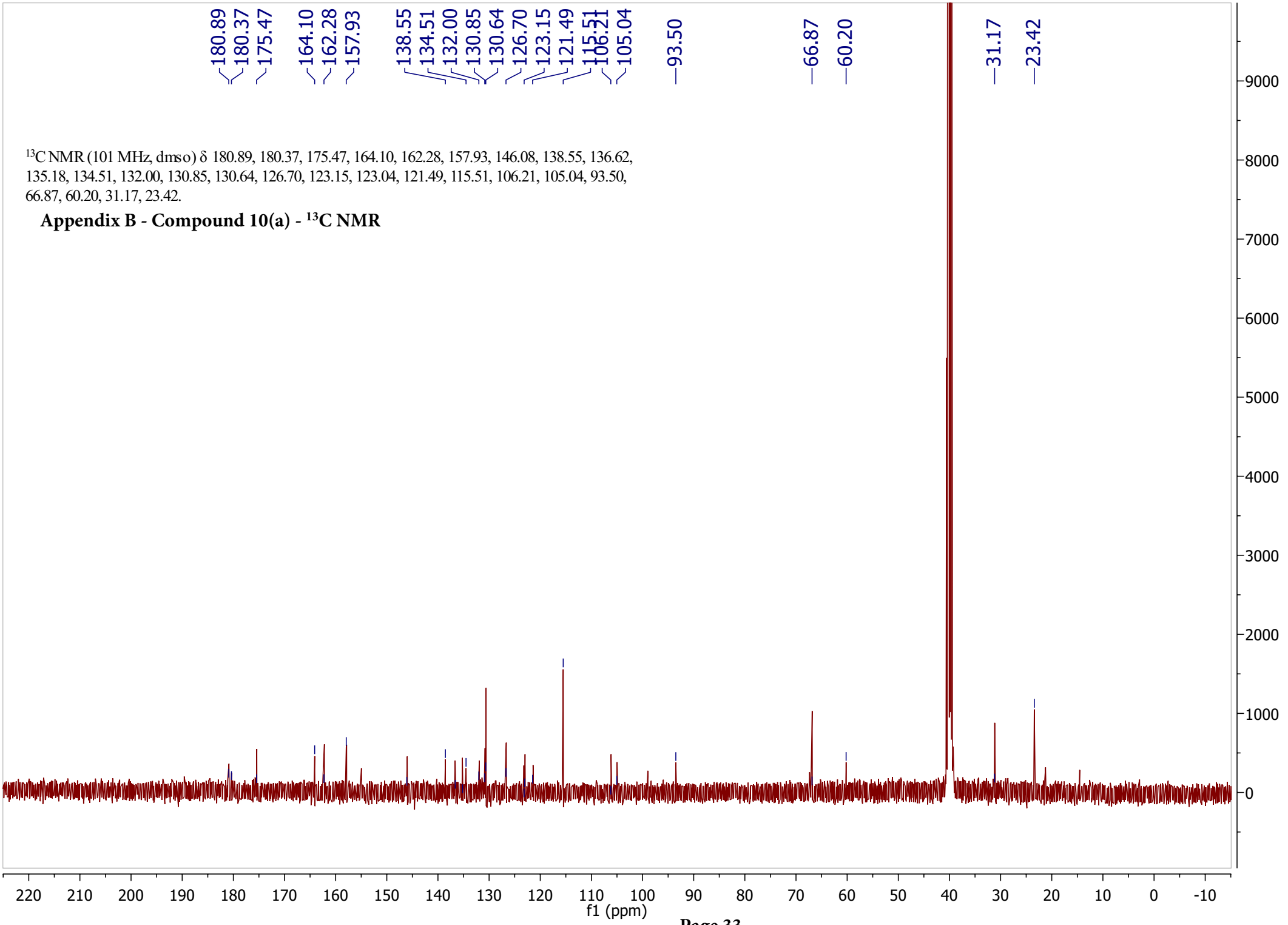

^{13}C NMR (101 MHz, dmso) δ 180.89, 180.37, 175.47, 164.10, 162.28, 157.93, 146.08, 138.55, 136.62, 135.18, 134.51, 132.00, 130.85, 130.64, 126.70, 123.15, 123.04, 121.49, 115.51, 106.21, 105.04, 93.50, 66.87, 60.20, 31.17, 23.42.

Appendix B - Compound 10(a) - ^{13}C NMR

^{1}H NMR (400 MHz, dmso) δ 12.98 (s, 1H), 9.65 (s, 1H), 8.70 (s, 1H), 8.47 – 8.34 (m, 2H), 8.14 (d, *J* = 8.4 Hz, 1H), 7.86 (d, *J* = 8.2 Hz, 2H), 7.59 (d, *J* = 8.5 Hz, 2H), 7.41 (d, *J* = 8.7 Hz, 2H), 6.84 (d, *J* = 8.6 Hz, 2H), 6.49 (s, 1H), 5.16 (s, 2H), 4.88 (s, 2H), 4.61 (s, 2H), 3.37 (s, 16H).

Appendix B - Compound 11(a) - ^{1}H NMR

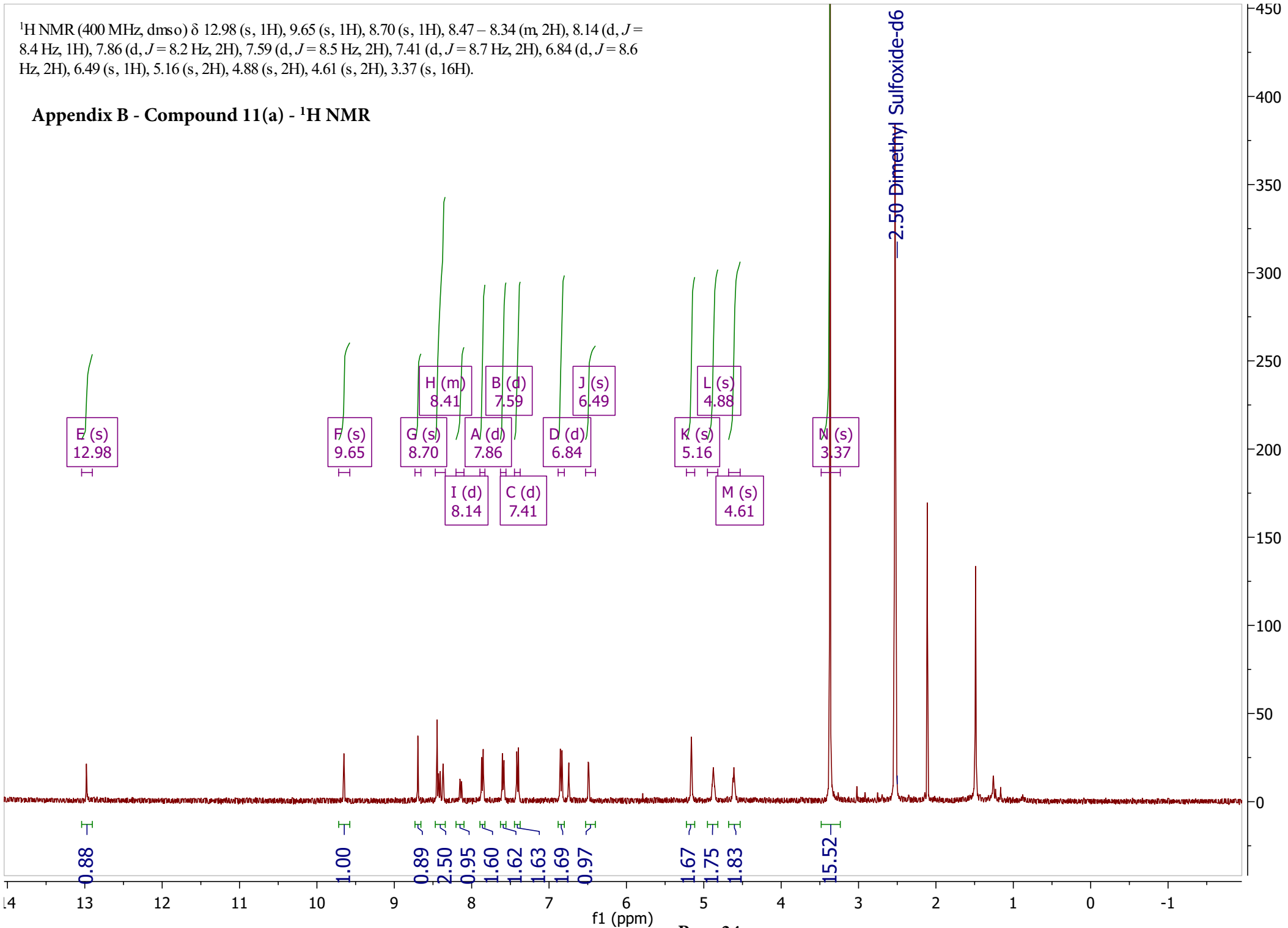

^{1}H NMR (400 MHz, cdcl$_3$) δ 12.83 (s, 1H), 8.11 (s, 1H), 7.97 (d, *J* = 10.0 Hz, 1H), 7.87 (d, *J* = 8.4 Hz, 1H), 7.78 (s, 1H), 7.52 (s, 1H), 7.31 (d, *J* = 8.5 Hz, 2H), 6.90 (d, *J* = 8.5 Hz, 2H), 6.32 (dd, *J* = 12.4, 2.2 Hz, 2H), 5.28 (s, 1H), 4.48 (s, 2H), 4.10 (s, 2H), 3.82 (s, 4H), 3.60 (t, *J* = 10.2 Hz, 23H), 3.35 (s, 2H), 2.75 (s, 2H), 2.61 (s, 2H), 1.75 (s, 4H), 1.48 (s, 5H).

Appendix B - Compound 9(b) - ^{1}H NMR

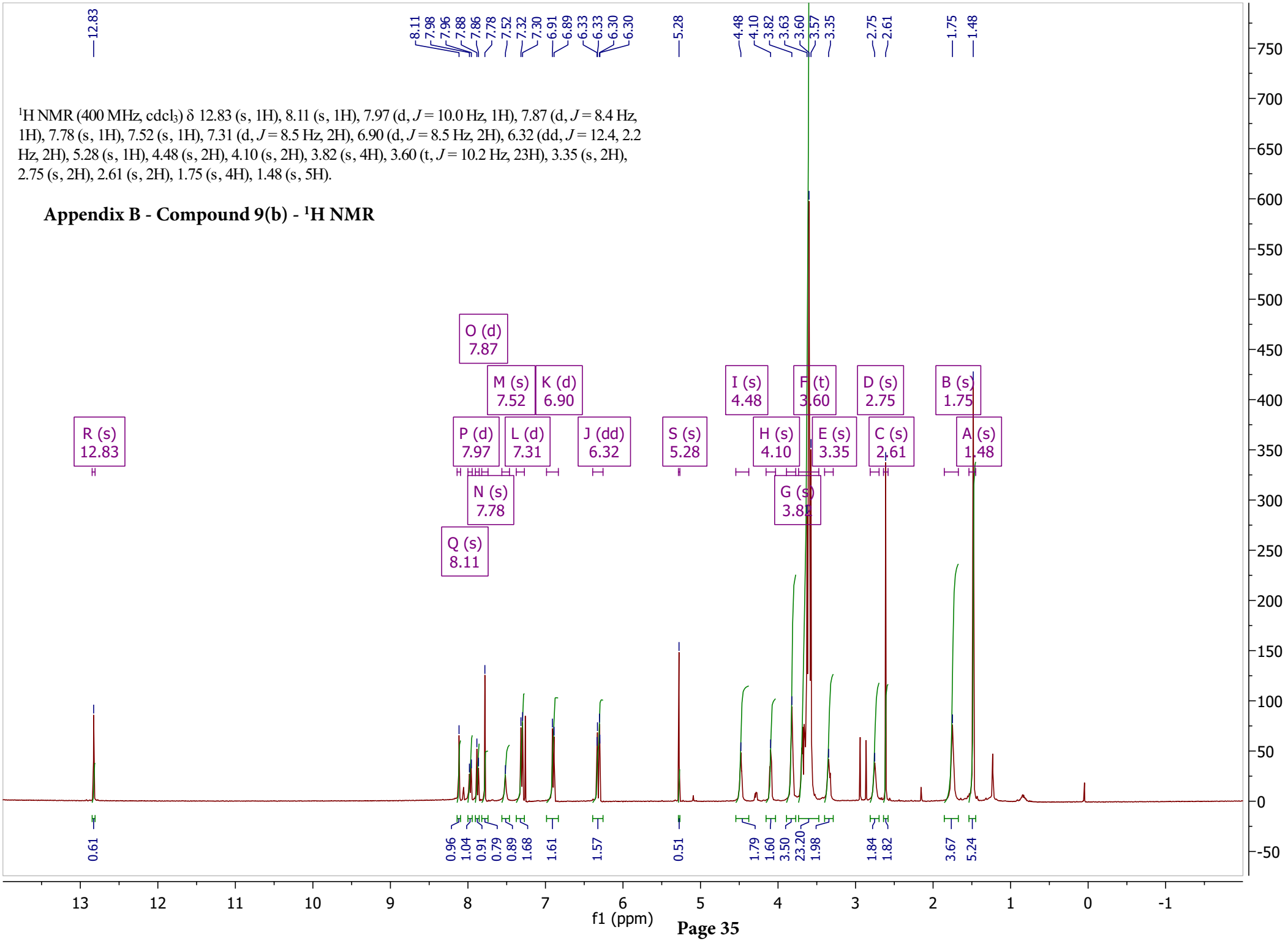

Appendix B - Compound 9(b) - ^{13}C NMR

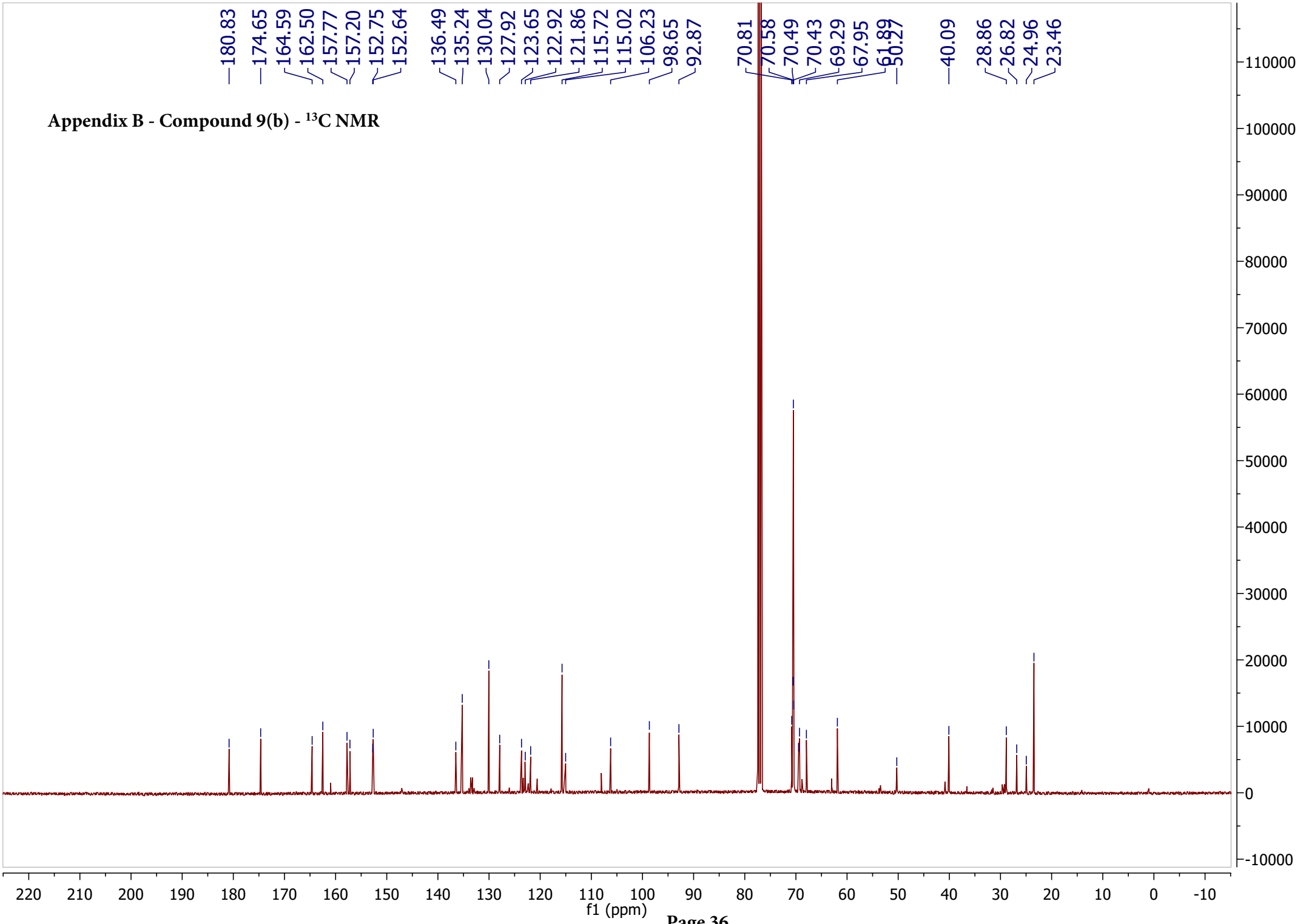

^{1}H NMR (400 MHz, cdcl$_3$) δ 12.83 (s, 1H), 8.12 (s, 1H), 7.99 (d, *J* = 16.0 Hz, 4H), 7.85 (d, *J* = 8.4 Hz, 1H), 7.76 (s, 1H), 7.40 – 7.29 (m, 4H), 6.90 (d, *J* = 8.5 Hz, 2H), 6.31 (d, *J* = 3.0 Hz, 2H), 4.60 (s, 2H), 4.07 (s, 2H), 3.90 (s, 2H), 3.81 (s, 2H), 3.63 (t, *J* = 20.5 Hz, 22H), 3.48 (s, 1H), 1.60 (s, 4H), 1.25 (s, 1H).

Appendix B - Compound 10(b) - ^{1}H NMR

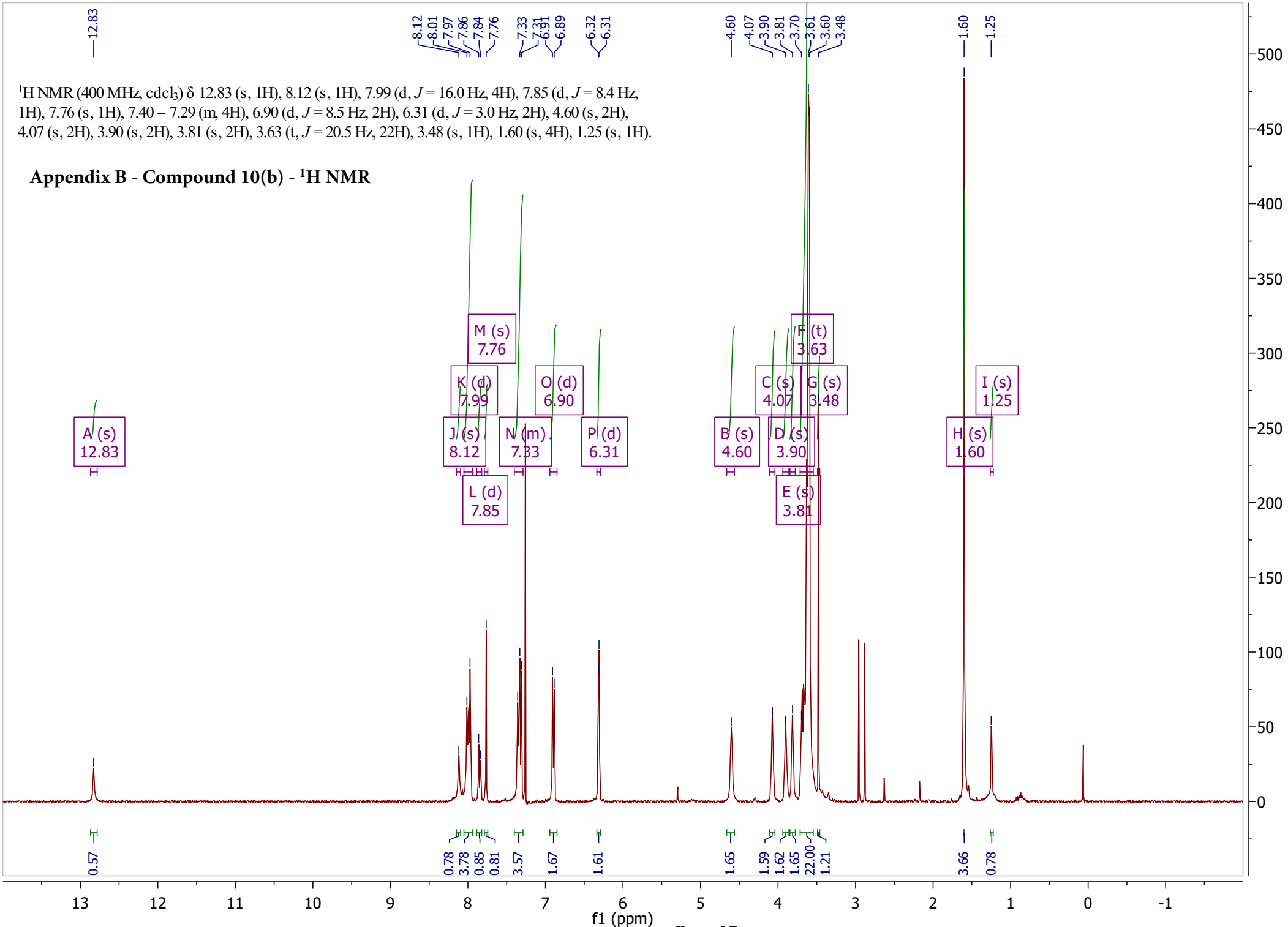

^{13}C NMR (101 MHz, cdcl$_3$) δ 179.94, 178.81, 173.97, 163.84, 161.55, 157.01, 155.87, 151.95, 145.15, 136.05, 134.38, 133.25, 132.71, 131.81, 131.58, 128.98, 125.91, 122.51, 121.38, 121.07, 119.70, 114.86, 113.73, 109.18, 105.23, 97.61, 91.93, 69.31, 68.17, 67.04, 65.60, 49.52, 22.91.

Appendix B - Compound 10(b) - ^{13}C NMR

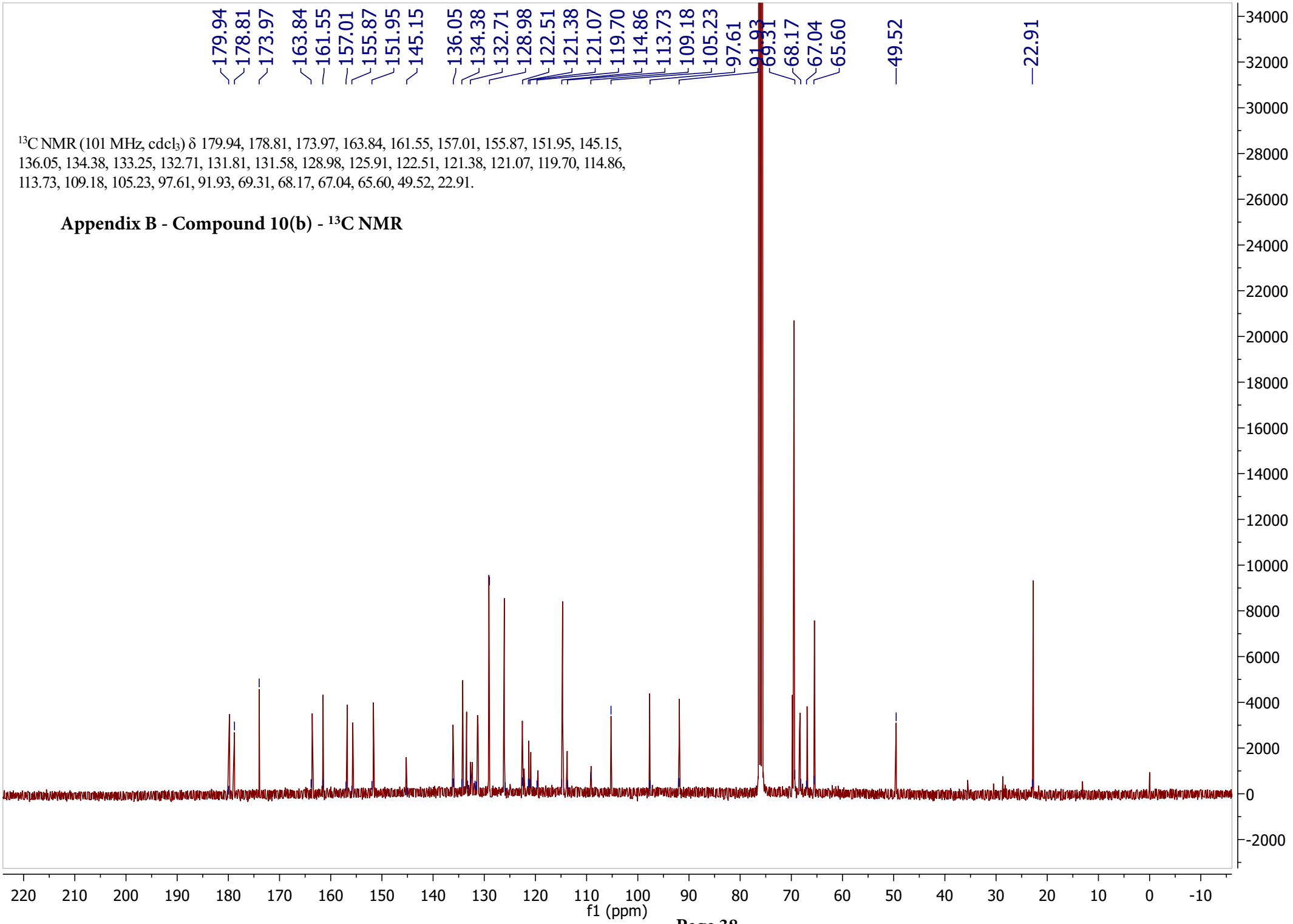

^{1}H NMR (400 MHz, cdcl$_3$) δ 12.83 (s, 1H), 8.04 (s, 1H), 8.00 – 7.92 (m, 2H), 7.83 (d, *J* = 7.9 Hz, 3H), 7.77 (s, 1H), 7.47 (d, *J* = 7.6 Hz, 2H), 7.32 (d, *J* = 8.4 Hz, 2H), 6.91 (d, *J* = 8.4 Hz, 2H), 6.32 (dd, *J* = 6.6, 2.1 Hz, 2H), 5.29 (s, 2H), 5.13 (s, 2H), 4.58 (s, 2H), 4.08 (s, 2H), 3.89 (s, 2H), 3.82 (s, 2H), 3.60 (t, *J* = 8.9 Hz, 23H), 1.46 (s, 5H), 1.24 (s, 1H).

Appendix B - Compound 11(b) - ^{1}H NMR

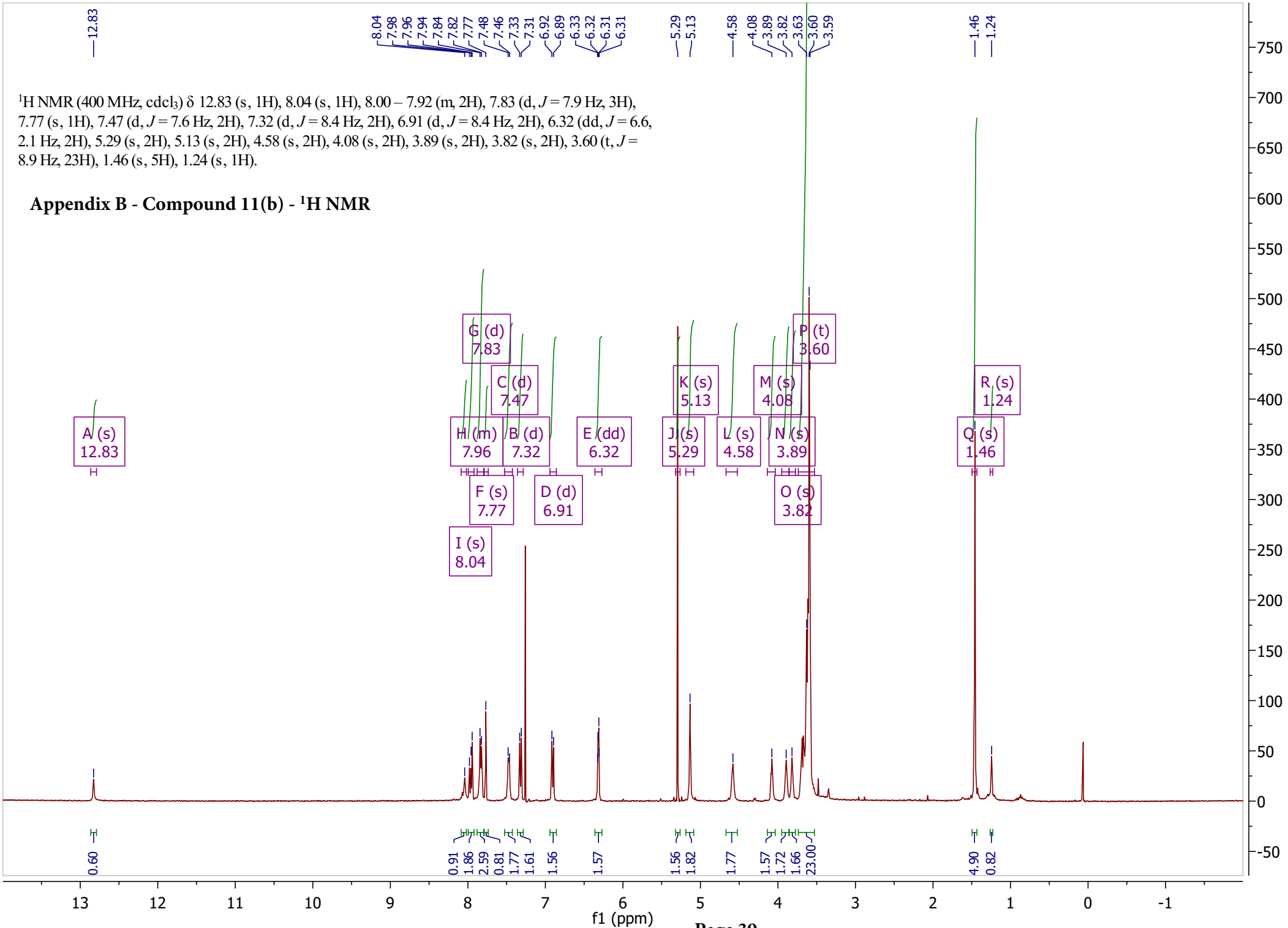

Appendix B - Compound 11(b) - ^{13}C NMR

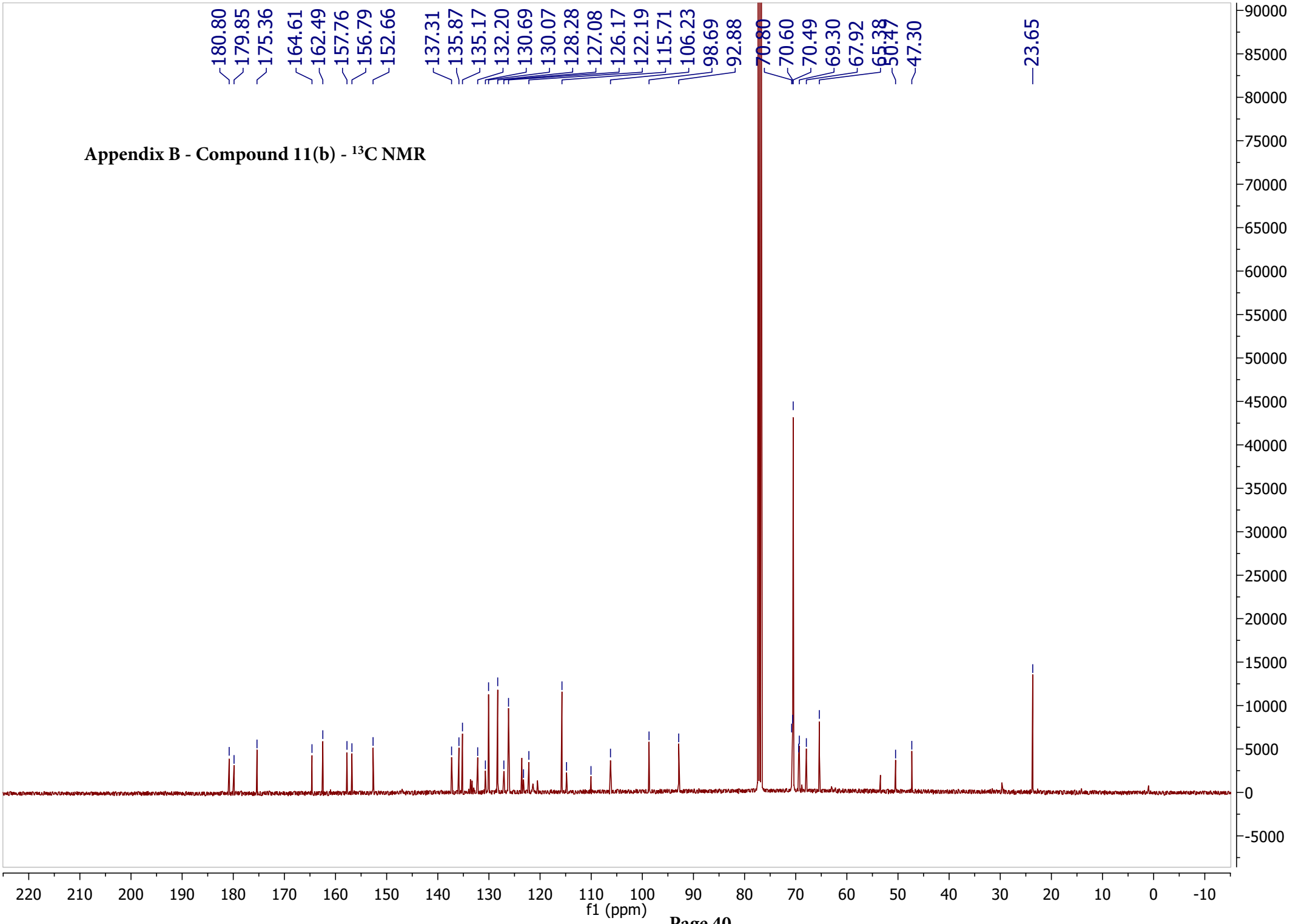

APPENDIX C

MASS SPECTROSCOPY DATA

This appendix contains mass spectroscopy data from all target compounds.

Appendix C - Compound 9(a)

YO140826-02 #79-112 RT: 1.86-2.65 AV: 34 NL: 1.33E7
T: FTMS + p ESI Full ms [150.00-2000.00]

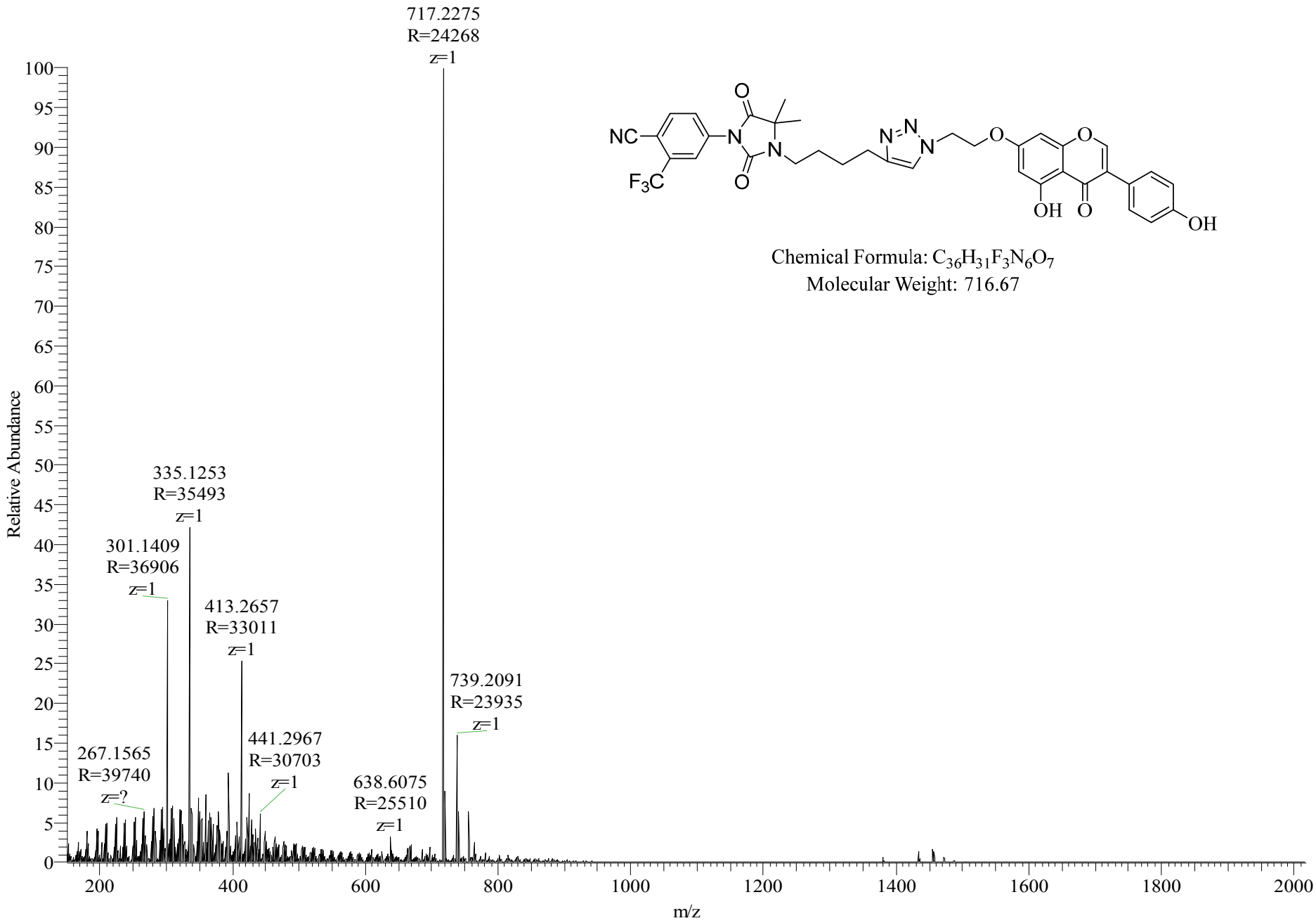

Chemical Formula: $C_{36}H_{31}F_3N_6O_7$
Molecular Weight: 716.67

YO140826-04 #81-120 RT: 1.91-2.84 AV: 40 NL: 2.56E6
T: FTMS + p ESI Full ms [150.00-2000.00]

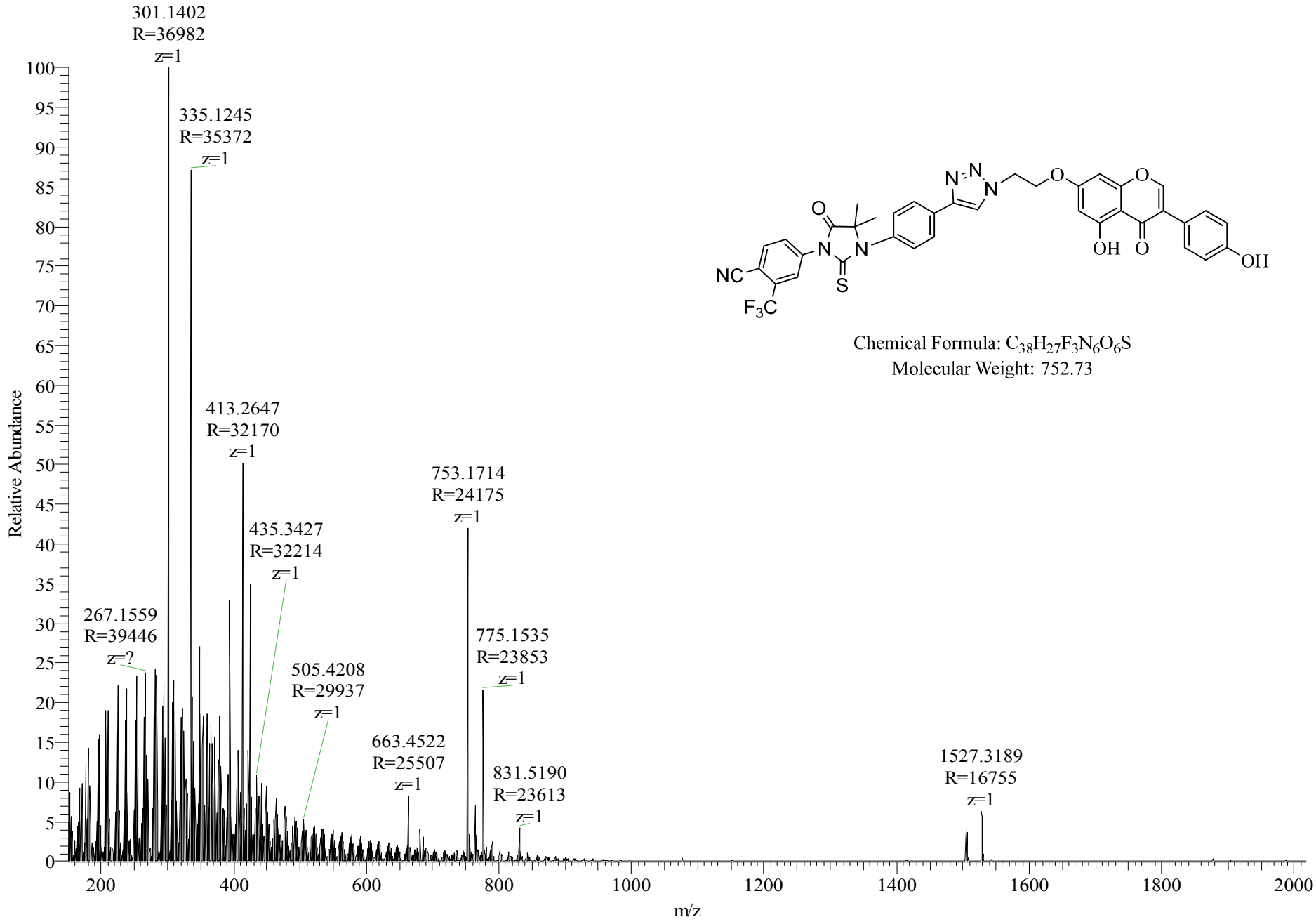

Chemical Formula: $C_{38}H_{27}F_3N_6O_6S$
Molecular Weight: 752.73

YO140911-02 #230-302 RT: 1.95-2.54 AV: 73 NL: 9.53E6
T: FTMS + p ESI Full ms [150.00-2000.00]

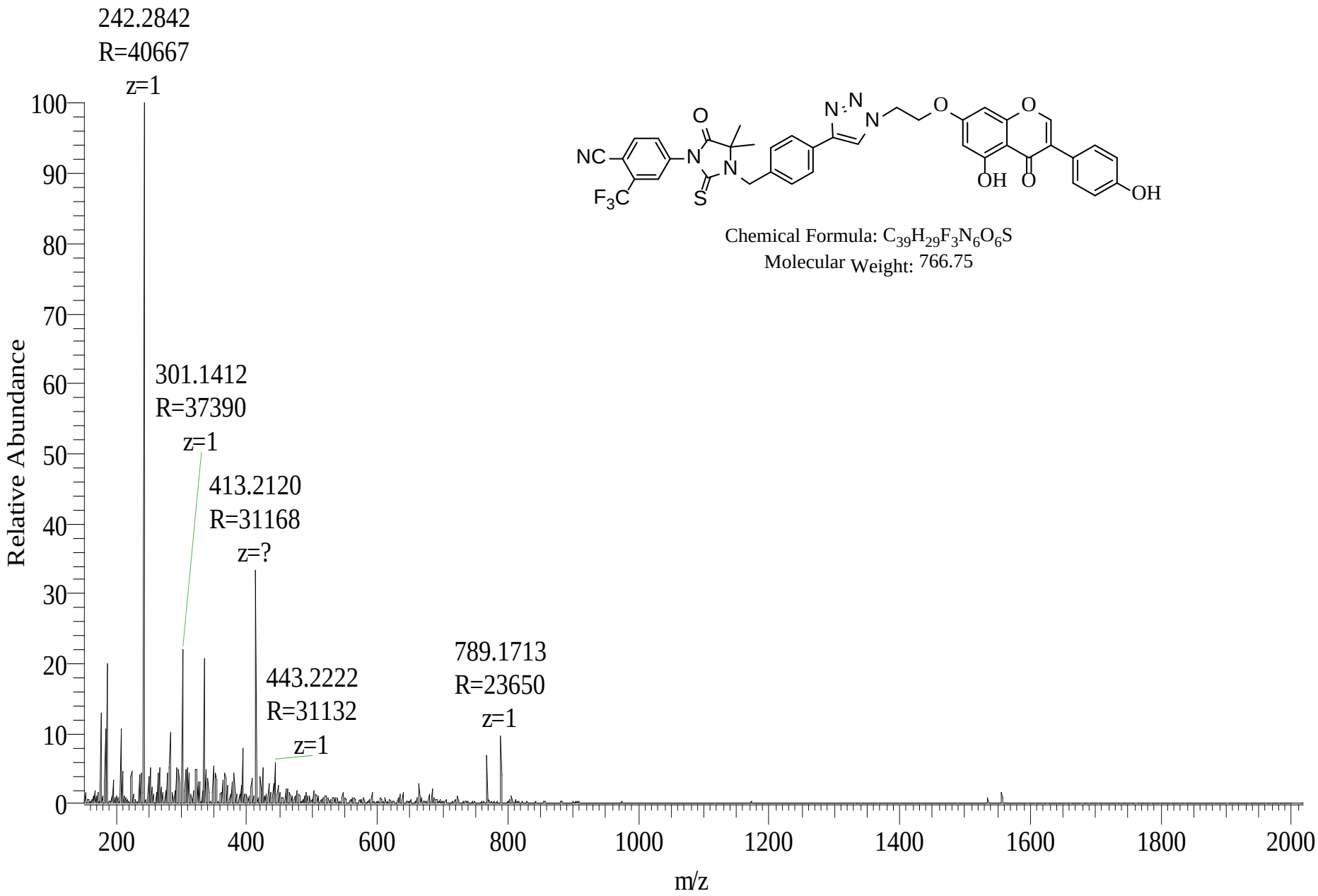

Chemical Formula: $C_{39}H_{29}F_3N_6O_6S$
Molecular Weight: 766.75

YO141023-01 #74-117 RT: 1.73-2.74 AV: 44 NL: 1.05E8
T: FTMS + p ESI Full ms [150.00-2000.00]

Appendix C - Compound 9(b)

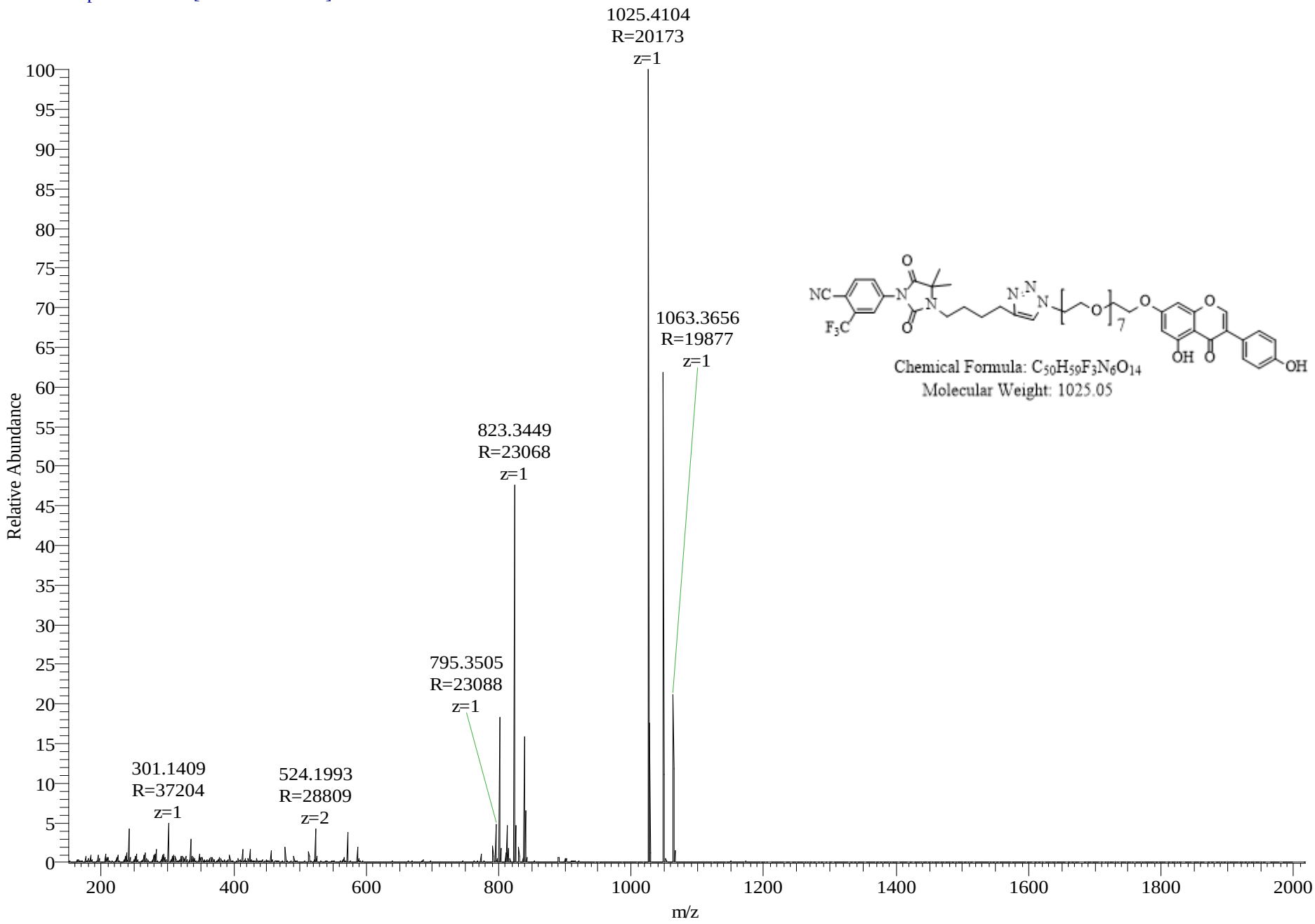

YO141023-02 #82-127 RT: 1.93-3.01 AV: 46 NL: 1.26E7
T: FTMS + p ESI Full ms [150.00-2000.00]

Appendix C - Compound 10(b)

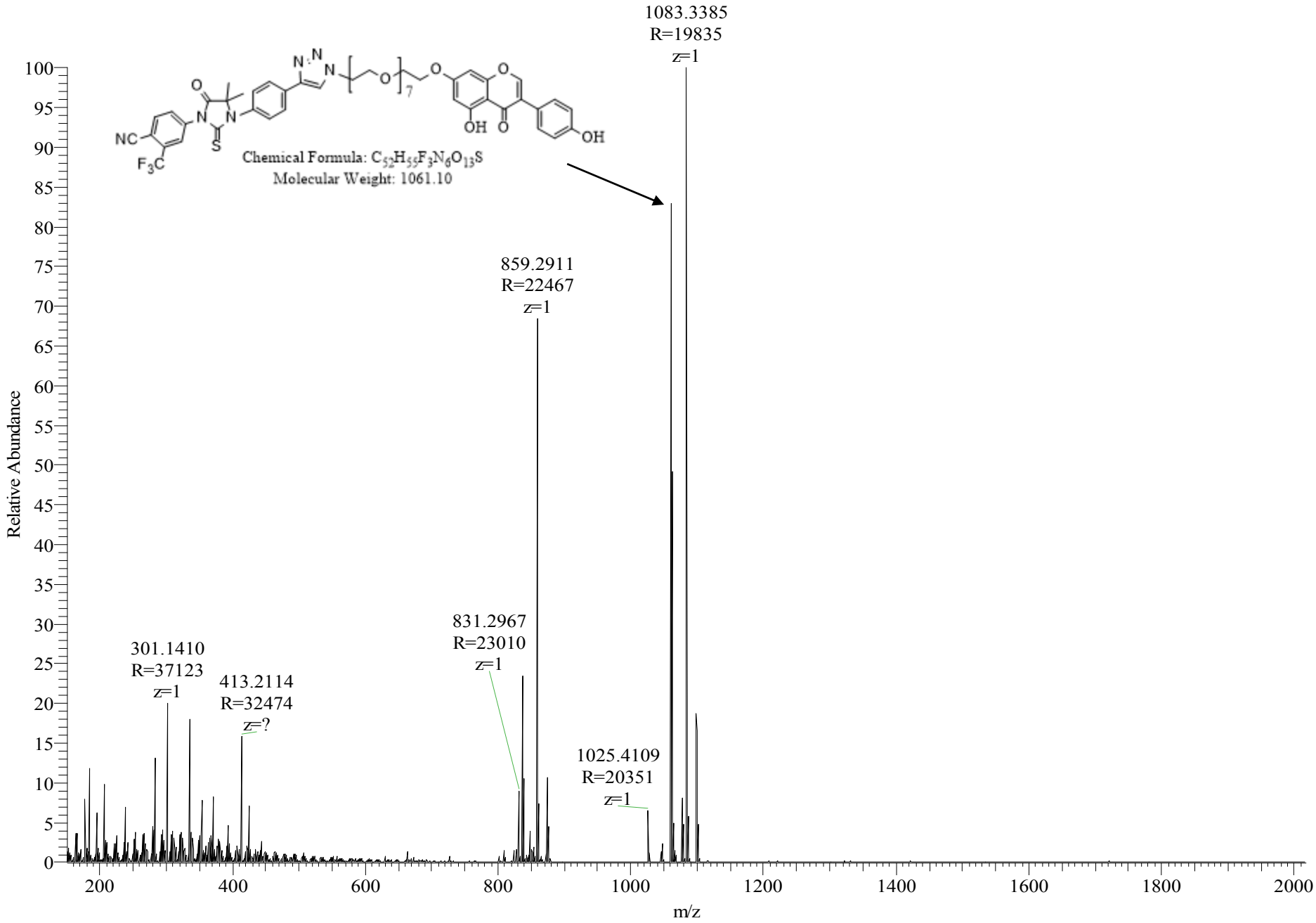

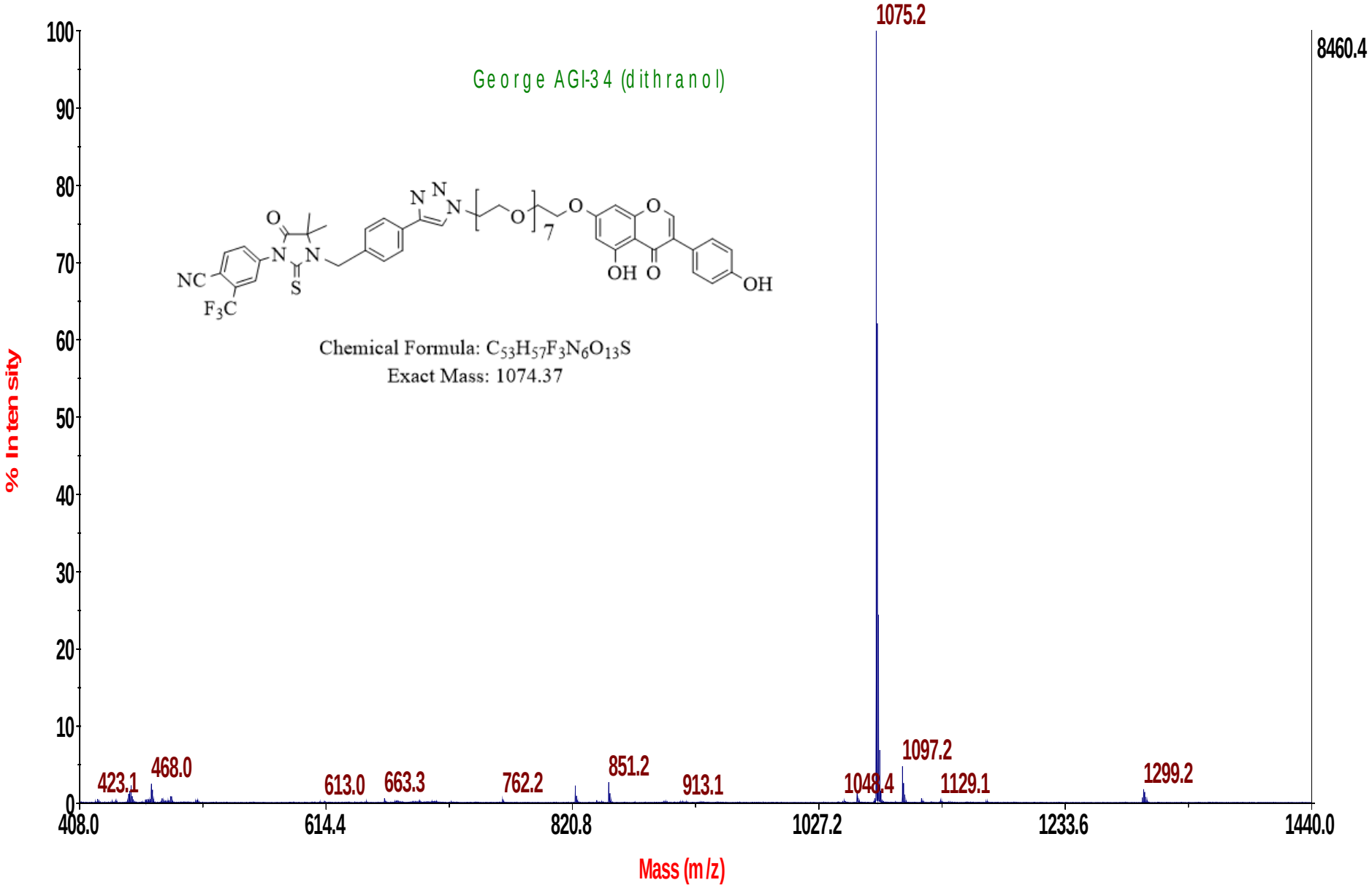
4700 Reflector Spec #1 MC [BP = 1075.2, 8460]
1075.2
8460.4
George AGI-34 (dithranol)
Chemical Formula: C53H57F3N6O13S
Exact Mass: 1074.37
% Intensity
Mass (m/z)
100
90
80
70
60
50
40
30
20
10
0
408.0
614.4
820.8
1027.2
1233.6
1440.0
423.1
468.0
613.0
663.3
762.2
851.2
913.1
1048.4
1097.2
1129.1
1299.2

REFERENCES

1. Centers for Disease Control and Prevention. *United States Cancer Statistics (USCS).* 2014; Available from: http://apps.nccd.cdc.gov/uscs/.

2. DeSantis, C.E., C.C. Lin, A.B. Mariotto, R.L. Siegel, K.D. Stein, J.L. Kramer, R. Alteri, A.S. Robbins, and A. Jemal, *Cancer Treatment and Survivorship Statistics, 2014.* CA: A Cancer Journal for Clinicians, 2014. **64**(4): p. 252-271.

3. Cronauer, M.V., W.A. Schulz, T. Burchardt, A.G. Anastasiadis, A. de la Taille, R. Ackermann, and M. Burchardt, *The androgen receptor in hormone-refractory prostate cancer: relevance of different mechanisms of androgen receptor signaling (Review).* Int J Oncol, 2003. **23**(4): p. 1095-102.

4. Dixon, R.A. and D. Ferreira, *Genistein.* Phytochemistry, 2002. **60**(3): p. 205-11.

5. Davis, J.N., O. Kucuk, and F.H. Sarkar, *Genistein inhibits NF-kappa B activation in prostate cancer cells.* Nutr Cancer, 1999. **35**(2): p. 167-74.

6. Jagadeesh, S., S. Kyo, and P.P. Banerjee, *Genistein represses telomerase activity via both transcriptional and posttranslational mechanisms in human prostate cancer cells.* Cancer Res, 2006. **66**(4): p. 2107-15.

7. Li, Y. and F.H. Sarkar, *Inhibition of nuclear factor kappaB activation in PC3 cells by genistein is mediated via Akt signaling pathway.* Clin Cancer Res, 2002. **8**(7): p. 2369-77.

8. Sasamura, H., A. Takahashi, J. Yuan, H. Kitamura, N. Masumori, N. Miyao, N. Itoh, and T. Tsukamoto, *Antiproliferative and antiangiogenic activities of genistein in human renal cell carcinoma.* Urology, 2004. **64**(2): p. 389-393.

9. Su, S.-J., T.-M. Yeh, W.-J. Chuang, C.-L. Ho, K.-L. Chang, H.-L. Cheng, H.-S. Liu, H.-L. Cheng, P.-Y. Hsu, and N.-H. Chow, *The novel targets for anti-angiogenesis of genistein on human cancer cells.* Biochemical Pharmacology, 2005. **69**(2): p. 307-318.

10. Vinall, R.L., K. Hwa, P. Ghosh, C.X. Pan, P.N. Lara, Jr., and R.W. de Vere White, *Combination treatment of prostate cancer cell lines with bioactive soy isoflavones and perifosine causes increased growth arrest and/or apoptosis.* Clin Cancer Res, 2007. **13**(20): p. 6204-16.

11. Gryder, B.E., M.J. Akbashev, M.K. Rood, E.D. Raftery, W.M. Meyers, P. Dillard, S. Khan, and A.K. Oyelere, *Selectively targeting prostate cancer with antiandrogen equipped histone deacetylase inhibitors.* ACS Chem Biol, 2013. **8**(11): p. 2550-60.

12. Corson, T.W., N. Aberle, and C.M. Crews, *Design and Applications of Bifunctional Small Molecules: Why Two Heads Are Better Than One.* ACS Chemical Biology, 2008. **3**(11): p. 677-692.

13. Schneekloth, A.R., M. Pucheault, H.S. Tae, and C.M. Crews, *Targeted intracellular protein degradation induced by a small molecule: En route to*

chemical proteomics. Bioorganic & Medicinal Chemistry Letters, 2008. **18**(22): p. 5904-5908.

14. Gustafson, J.L., T.K. Neklesa, C.S. Cox, A.G. Roth, D.L. Buckley, H.S. Tae, T.B. Sundberg, D.B. Stagg, J. Hines, D.P. McDonnell, J.D. Norris, and C.M. Crews, *Small-Molecule-Mediated Degradation of the Androgen Receptor through Hydrophobic Tagging.* Angew Chem Int Ed Engl, 2015. **54**(33): p. 9659-62.

15. Lamb, A.D., C.E. Massie, and D.E. Neal, *The transcriptional programme of the androgen receptor (AR) in prostate cancer.* BJU Int, 2014. **113**(3): p. 358-66.

16. Bennett, N.C., R.A. Gardiner, J.D. Hooper, D.W. Johnson, and G.C. Gobe, *Molecular cell biology of androgen receptor signalling.* Int J Biochem Cell Biol, 2010. **42**(6): p. 813-27.

17. Chen, Y., N.J. Clegg, and H.I. Scher, *Anti-androgens and androgen-depleting therapies in prostate cancer: new agents for an established target.* Lancet Oncol, 2009. **10**(10): p. 981-91.

18. Shafi, A.A., A.E. Yen, and N.L. Weigel, *Androgen receptors in hormone-dependent and castration-resistant prostate cancer.* Pharmacol Ther, 2013. **140**(3): p. 223-38.

19. Brooke, G.N. and C.L. Bevan, *The Role of Androgen Receptor Mutations in Prostate Cancer Progression.* Current Genomics, 2009. **10**(1): p. 18-25.

20. Waltering, K.K., A. Urbanucci, and T. Visakorpi, *Androgen receptor (AR) aberrations in castration-resistant prostate cancer.* Mol Cell Endocrinol, 2012. **360**(1-2): p. 38-43.

21. Steinkamp, M.P., O.A. O'Mahony, M. Brogley, H. Rehman, E.W. Lapensee, S. Dhanasekaran, M.D. Hofer, R. Kuefer, A. Chinnaiyan, M.A. Rubin, K.J. Pienta, and D.M. Robins, *Treatment-dependent androgen receptor mutations in prostate cancer exploit multiple mechanisms to evade therapy.* Cancer Res, 2009. **69**(10): p. 4434-42.

22. Taplin, M.E., G.J. Bubley, Y.J. Ko, E.J. Small, M. Upton, B. Rajeshkumar, and S.P. Balk, *Selection for androgen receptor mutations in prostate cancers treated with androgen antagonist.* Cancer Res, 1999. **59**(11): p. 2511-5.

23. Korpal, M., J.M. Korn, X. Gao, D.P. Rakiec, D.A. Ruddy, S. Doshi, J. Yuan, S.G. Kovats, S. Kim, V.G. Cooke, J.E. Monahan, F. Stegmeier, T.M. Roberts, W.R. Sellers, W. Zhou, and P. Zhu, *An F876L mutation in androgen receptor confers genetic and phenotypic resistance to MDV3100 (enzalutamide).* Cancer Discov, 2013. **3**(9): p. 1030-43.

24. Taplin, M.-E., G.J. Bubley, T.D. Shuster, M.E. Frantz, A.E. Spooner, G.K. Ogata, H.N. Keer, and S.P. Balk, *Mutation of the Androgen-Receptor Gene in Metastatic Androgen-Independent Prostate Cancer.* New England Journal of Medicine, 1995. **332**(21): p. 1393-1398.

25. Culig, Z., A. Hobisch, M.V. Cronauer, A.C. Cato, A. Hittmair, C. Radmayr, J. Eberle, G. Bartsch, and H. Klocker, *Mutant androgen receptor detected in an advanced-stage prostatic carcinoma is activated by adrenal androgens and progesterone.* Mol Endocrinol, 1993. **7**(12): p. 1541-50.

26. Zhao, X.Y., P.J. Malloy, A.V. Krishnan, S. Swami, N.M. Navone, D.M. Peehl, and D. Feldman, *Glucocorticoids can promote androgen-independent growth of prostate cancer cells through a mutated androgen receptor.* Nat Med, 2000. **6**(6): p. 703-6.

27. Linja, M.J., K.J. Savinainen, O.R. Saramaki, T.L. Tammela, R.L. Vessella, and T. Visakorpi, *Amplification and overexpression of androgen receptor gene in hormone-refractory prostate cancer.* Cancer Res, 2001. **61**(9): p. 3550-5.

28. Tran, C., S. Ouk, N.J. Clegg, Y. Chen, P.A. Watson, V. Arora, J. Wongvipat, P.M. Smith-Jones, D. Yoo, A. Kwon, T. Wasielewska, D. Welsbie, C.D. Chen, C.S. Higano, T.M. Beer, D.T. Hung, H.I. Scher, M.E. Jung, and C.L. Sawyers, *Development of a second-generation antiandrogen for treatment of advanced prostate cancer.* Science, 2009. **324**(5928): p. 787-90.

29. Gartrell, B.A. and F. Saad, *Abiraterone in the management of castration-resistant prostate cancer prior to chemotherapy.* Ther Adv Urol, 2015. **7**(4): p. 194-202.

30. Attard, G., A.H. Reid, T.A. Yap, F. Raynaud, M. Dowsett, S. Settatree, M. Barrett, C. Parker, V. Martins, E. Folkerd, J. Clark, C.S. Cooper, S.B. Kaye, D. Dearnaley, G. Lee, and J.S. de Bono, *Phase I clinical trial of a selective inhibitor*

of CYP17, abiraterone acetate, confirms that castration-resistant prostate cancer commonly remains hormone driven. J Clin Oncol, 2008. **26**(28): p. 4563-71.

31. Cao, C., S.R. Li, X. Dai, Y.Q. Chen, Z. Feng, X. Qin, Y. Zhao, and J. Wu, *[The effects of genistein on tyrosine protein kinase-mitogen activated protein kinase signal transduction pathway in hypertrophic scar fibroblasts]*. Zhonghua Shao Shang Za Zhi, 2008. **24**(2): p. 118-21.

32. Majid, S., N. Kikuno, J. Nelles, E. Noonan, Y. Tanaka, K. Kawamoto, H. Hirata, L.C. Li, H. Zhao, S.T. Okino, R.F. Place, D. Pookot, and R. Dahiya, *Genistein induces the p21WAF1/CIP1 and p16INK4a tumor suppressor genes in prostate cancer cells by epigenetic mechanisms involving active chromatin modification.* Cancer Res, 2008. **68**(8): p. 2736-44.

33. Kikuno, N., H. Shiina, S. Urakami, K. Kawamoto, H. Hirata, Y. Tanaka, S. Majid, M. Igawa, and R. Dahiya, *Genistein mediated histone acetylation and demethylation activates tumor suppressor genes in prostate cancer cells.* Int J Cancer, 2008. **123**(3): p. 552-60.

34. Davis, J.N., N. Muqim, M. Bhuiyan, O. Kucuk, K.J. Pienta, and F.H. Sarkar, *Inhibition of prostate specific antigen expression by genistein in prostate cancer cells.* Int J Oncol, 2000. **16**(6): p. 1091-7.

35. Davis, J.N., O. Kucuk, and F.H. Sarkar, *Expression of prostate-specific antigen is transcriptionally regulated by genistein in prostate cancer cells.* Mol Carcinog, 2002. **34**(2): p. 91-101.

36. Basak, S., D. Pookot, E.J. Noonan, and R. Dahiya, *Genistein down-regulates androgen receptor by modulating HDAC6-Hsp90 chaperone function.* Mol Cancer Ther, 2008. **7**(10): p. 3195-202.

37. Phillip, C.J., C.K. Giardina, B. Bilir, D.J. Cutler, Y.H. Lai, O. Kucuk, and C.S. Moreno, *Genistein cooperates with the histone deacetylase inhibitor vorinostat to induce cell death in prostate cancer cells.* BMC Cancer, 2012. **12**: p. 145.

38. Neklesa, T.K., H.S. Tae, A.R. Schneekloth, M.J. Stulberg, T.W. Corson, T.B. Sundberg, K. Raina, S.A. Holley, and C.M. Crews, *Small-molecule hydrophobic tagging–induced degradation of HaloTag fusion proteins.* Nat Chem Biol, 2011. **7**(8): p. 538-543.

39. Teutsch, G., F. Goubet, T. Battmann, A. Bonfils, F. Bouchoux, E. Cerede, D. Gofflo, M. Gaillard-Kelly, and D. Philibert, *Non-steroidal antiandrogens: synthesis and biological profile of high-affinity ligands for the androgen receptor.* J Steroid Biochem Mol Biol, 1994. **48**(1): p. 111-9.

40. Gryder, B.E., M.J. Akbashev, M.K. Rood, E.D. Raftery, W.M. Meyers, P. Dillard, S. Khan, and A.K. Oyelere, *Selectively Targeting Prostate Cancer with Antiandrogen Equipped Histone Deacetylase Inhibitors.* ACS chemical biology, 2013. **8**(11): p. 10.1021/cb400542w.

41. Grynkiewicz, G., O. Zegrocka-Stendel, W. Pucko, J. Ramza, A. Kościelecka, W. Kołodziejski, and K. Woźniak, *X-ray and 13C CP MAS investigations of structure*

of two genistein derivatives. Journal of Molecular Structure, 2004. **694**(1–3): p. 121-129.

42. Jiao, L., Q. Qiu, B. Liu, T. Zhao, W. Huang, and H. Qian, *Design, synthesis and evaluation of novel triazole core based P-glycoprotein-mediated multidrug resistance reversal agents.* Bioorg Med Chem, 2014. **22**(24): p. 6857-66.

43. Dreaden, E.C., I.O. Raji, L.A. Austin, S. Fathi, S.C. Mwakwari, W.H.t. Humphries, B. Kang, A.K. Oyelere, and M.A. El-Sayed, *P-glycoprotein-dependent trafficking of nanoparticle-drug conjugates.* Small, 2014. **10**(9): p. 1719-23.

44. Bock, V.D., H. Hiemstra, and J.H. van Maarseveen, *CuI-Catalyzed Alkyne–Azide "Click" Cycloadditions from a Mechanistic and Synthetic Perspective.* European Journal of Organic Chemistry, 2006. **2006**(1): p. 51-68.

45. Onozawa, M., K. Fukuda, M. Ohtani, H. Akaza, T. Sugimura, and K. Wakabayashi, *Effects of soybean isoflavones on cell growth and apoptosis of the human prostatic cancer cell line LNCaP.* Jpn J Clin Oncol, 1998. **28**(6): p. 360-3.

46. Zhao, R., N. Xiang, F.E. Domann, and W. Zhong, *Effects of selenite and genistein on G2/M cell cycle arrest and apoptosis in human prostate cancer cells.* Nutr Cancer, 2009. **61**(3): p. 397-407.

47. Lucki, N.C. and M.B. Sewer, *Genistein stimulates MCF-7 breast cancer cell growth by inducing acid ceramidase (ASAH1) gene expression.* J Biol Chem, 2011. **286**(22): p. 19399-409.

48. Matsukawa, Y., N. Marui, T. Sakai, Y. Satomi, M. Yoshida, K. Matsumoto, H. Nishino, and A. Aoike, *Genistein arrests cell cycle progression at G2-M.* Cancer Res, 1993. **53**(6): p. 1328-31.

49. Shen, J.C., R.D. Klein, Q. Wei, Y. Guan, J.H. Contois, T.T. Wang, S. Chang, and S.D. Hursting, *Low-dose genistein induces cyclin-dependent kinase inhibitors and G(1) cell-cycle arrest in human prostate cancer cells.* Mol Carcinog, 2000. **29**(2): p. 92-102.